A COMPUTING SYSTEM FOR THE DESIGN-POINT PERFORMANCE OF AXIAL TURBINES

A Thesis Submitted
In Partial Fulfilment of the Requirements
for the Degree of
MASTER OF TECHNOLOGY

By
T. R. GOVINDAN

to the

DEPARTMENT OF AERONAUTICAL ENGINEERING
INDIAN INSTITUTE OF TECHNOLOGY KANPUR
JANUARY, 1978

CERTIFICATE

This is to certify that the thesis entitled "A Computing System for the design-point performance of Axial turbines" by T.R. Govindan is a record of work carried out under my supervision and has not been submitted elsewhere for a degree.

Dated : 3rd JAN 1978

Dr. R.K. Sullerey
Asst. Prof., Dept. of Aeronautical Engg
I.I.T. Kanpur

CERTIFICATE

This is to certify that the thesis entitled "A Computing System for the design-point performance of Axial turbines" by T.R. Govindan is a record of work carried out under my supervision and has not been submitted elsewhere for a degree.

Dated : 3rd JAN 1978

Dr. R.K. Sullerey
Asst. Prof., Dept. of Aeronautical Engg.
I.I.T. Kanpur

ACKNOWLEDGEMENTS

The author wishes to express his deep sense of gratitude to Dr. R.K. Sullorey for his guidance and encouragement throughout the course of this work.

Acknowledgements are also due to his friends, to Mr. Pankaj Kumar for proof reading, and to Mr. G.L. Misra for his excellent typing of the manuscript.

TABLE OF CONTENTS

ABSTRACT

Streamline curvature and the matrix through flow methods attempt to model a real flow in a turbomachine by a combination of an axisymmetric, inviscid flow model and a cascade loss model. The success of flow predictions depend on the adequacy of the loss model. The present work describes an application of streamline curvature method to predict the performance of highly loaded multi- and single stage turbines using different loss model. A loss model has been proposed in this work which not only evaluates the overall loss level in a turbine but also distributes these losses radially in the turbine annulus in a proper manner.

The predicted results using this loss model compare very well with the experimental measurements for the above turbines. Results obtained using other loss models have also been compared with those of present loss model.

Nomenclature

Symbol	Description
b_c	Blade chord
b_h	Blade height
b_t	Blade thickness
c_p	Specific heat at constant pressure
h	Enthalpy
j	Streamline index
M	Mach number
m	Meridional coordinate
P	Nondimensional power function
p	Static pressure
p_o	Stagnation pressure
R	Gas constant
r	Radius
r_m	Streamline radius of curvature
S	Entropy
T	Static temperature
T_o	Total temperature
t	Time
u	Blade speed
V	Velocity
W	Relative velocity
w	Mass flow
x	Axial coordinate

Symbol	Description
Y	Pressure-loss-coefficient
β	Flow angle
γ	Specific heat ratio
δ	Deflection
δ_1	Initial boundary layer thickness
η_R	Rotor isentropic efficiency
η_S	Stage isentropic efficiency
ρ	Density
ω	Angular velocity
μ	Mixing coefficients
ϕ	Streamline slope
θ	Tangential coordinate

Subscript	Description
ex	Exit
h	Hub
in	Inlet
m	Meridional component
N	Stator
R	Rotor
r	Radial component
T	Total
u	Tangential component
x	Axial component
0	Stage inlet

Subscript	Description
1	Stator exit/rotor inlet
2	Stage exit

Superscript	Description
'	Relative to the rotor

LIST OF FIGURES

CHAPTER 1

INTRODUCTION

The first step in the prediction of the performance of a turbomachine is to analyse the flow in it. The internal flow in a turbomachine is, in general, three dimensional, time dependent, and viscous and thus extremely complex to analyse. In addition, the flow is affected by such factors as tip clearance, coolant injection (in case of turbines) and by irregularities in the machine boundaries.

Due to the complex nature of the flow, a solution of the flow equations taking most of the above flow features into account simultaneously is a formidable task. Efforts at obtaining an analytical solution to the flow problem, in the past, have been made by making approximations that simplify the flow equations and permit the use of two-dimensional techniques for the solution. Some of these approximations are :

(1) The flow is assumed to be inviscid and steady

(2) Calculation is confined to those regions of the turbomachine where the axisymmetry assumption is likely to be valid, such as 'duct flows' between blade rows.

(3) Flow in the blade rows is taken to be circumferentially periodic with a period equal to the blade spacing.

(4) In analysing the blade-to-blade flow in a rotating blade row, a frame of reference fixed to the rotating blade is chosen and the flow is assumed steady with respect to it.

(5) Boundary layers are dealt with separately and their effect on available flow area, flow deflection, and irreversible losses are incorporated into an otherwise inviscid calculation.

As first shown by Wu (1), the three-dimensional inviscid flow in a turbomachine can be separated into two simpler but interrelated two-dimensional flows. One is the 'blade-to-blade' flow which occurs on a stream surface containing the tangential direction and describes the turning effect of the blade. The other is the meridional flow which occurs on a stream surface containing locally the radial and axial flow directions and describing the radial equilibrium of the flow. Figure 1 gives a representation of the blade-to-blade and meridional flows. This splitting of the three-dimensional flow into two two-dimensional flows has been fundamental to the success of turbomachine performance calculations.

The present work is concerned with the solution of the meridional flow problem to predict the performance of an axial flow turbine.

1.1 Methods for solving the meridional flow problem - A review

1.1.1 Matrix Through Flow Method (MTFM)

The method involves the solution for the stream function on a curvilinear grid on the meridional plane. The technique involves covering the region of interest with a fixed irregular grid and writing a finite difference approximation to the principal equation, given below, at every interior grid point.

$$\frac{\partial^2\psi}{\partial x^2} + \frac{\partial^2\psi}{\partial y^2} = q(x,y, \frac{\partial\psi}{\partial x} , \frac{\partial\psi}{\partial y}) \qquad (1.1)$$

This will result in an algebraic equation for every interior grid point in terms of the stream function at that and neighbouring points. This system of equations can be expressed in matrix form as

$$[A]\ [\psi] = [Q] \qquad (1.2)$$

where $[A]$ is the coefficient matrix derived by replacing the differential operator $\nabla^2( )$, $[\psi]$ is the vector of unknown stream function values, and $[Q]$ is the vector of quantities $q(x,y)$ from equation (1.1) and the boundary values.

Since the right hand side of equation (1.2) is a function of ψ and its derivatives, the system of equations is non-linear and must be solved iteratively, by first estimating $[\psi]$, computing $[Q]$, and then repeatedly

solving equation (1.2) for $[\psi]$. The value of $[Q]$ is improved in each iteration using the previous value of $[\psi]$.

This method of solution was first implemented by Marsh (2). Biniaris (3) has improved upon the formulation of the equations by incorporating the concept of a 'representative stream surface' and solving for the stream function on this surface. The blade forces were determined as that required to keep the flow in the surface. This method improves the solution for blades with lean.

Katsanis (4) has used the matrix method for obtaining subsonic solutions on a mid-channel surface in axial and mixed flow turbomachines.

Bosman and Marsh (5) have made further modifications to the formulation of the problem by writing the governing equation in a direction normal to the plane containing the velocity and body force vectors. By this, they are able to eliminate the body force terms from the equation. Furthermore, Bosman and Marsh (5) have introduced a dissipative force term in the governing equation to remove an inconsistency in the formulation by the introduction of a loss model.

1.1.2 The Finite Element Method

The formulation of the equations in this method is the same as that of the Matrix method. However, instead of using finite-differencing techniques as in the Matrix method,

the Finite Element method is used in solving the governing equations. Hirsch and Warzee (6) and Hirsch (7) have described the method in detail. The method is comparatively new and in the process of development and therefore yet to establish itself in turbomachine performance calculations.

1.1.3 The Streamline Curvature Method (SCM)

In the strea mline curvature method, the radial component of the Navier-Stokes equations is expressed in terms of the fluid properties and streamline geometry and solved in a specified direction, either along a quasi-orthogonal or a radial line, for the meridional velocity. The form of the equation solved for an arbitrary quasi-orthogonal direction s, is given by :

$$\frac{dV_m}{ds} = \left[C_1(s)\right] \frac{1}{V_m} - \left[C_2(s,V_m)\right] V_m \qquad (1.3)$$

where C_1 and C_2 are coefficients which are functions of the orthogonal direction, s, and the meridional velocity, V_m.

Since equation (1.3) requires a constant of integration, it must be solved in conjunction with the continuity equation, for the velocity along specified quasi-orthogonals.

Thus, there are two levels of iteration in the streamline curvature method, the outer iteration changes the streamline position based on the velocity distribution at each station,

and the inner iteration computes a velocity distribution which satisfies the continuity condition at each specified quasi-orthogonal.

Smith (8) has derived the exact radial equilibrium equation in a form suitable for the streamline curvature method. The equation has been derived by circumferential averaging of the flow variables in the momentum equations.

Novak (9) has described in detail the process of solving the meridional flow problem using the streamline curvature method. He has derived the governing radial equilibrium equation from the radial momentum equation of an inviscid flow by making use of the axisymmetry approximation. Novak has also discussed the problem of a non-axisymmetric computation which is necessary when computations are to be made within a blade row where the axisymmetry assumption is not valid. When such a computation is attempted, terms involving derivatives in the circumferential direction occur in the equations and the handling of these terms poses formidable problems.

The streamline curvature method for the off-design analysis of axial flow compressors has been implemented by Jansen and Moffat (10). The estimation of losses was accomplished by using cascade correlations developed by Mellor and Lieblin (11). Corrections have also been made for

the effects of streamline slope, axial velocity variations, blade thickness, and Mach numbers on the correlations. The paper is a pointer to the use and suitability of the streamline curvature method in turbomachine computations.

Frost (12) has improved upon the method so as to be able to make computations within blade rows. This has been achieved by using the concept of a 'mean stream surface' developed for the Matrix method. The flow equations have been derived on this stream surface and the blade forces determined as that required to keep the flow in the surface. Frost has called this method the 'streamline curvature through-flow method'. Losses have been accounted for by prescribing efficiencies for each blade row.

In a more sophisticated analysis, Novak and Bearsley (13) have obtained a 'nearly three-dimensional' solution to the flow in a turbomachine by using the streamline curvature method and iterating between the solutions obtained on the blade-to-blade and meridional planes. Computations can be carried out within blade rows with lean and twist. However the analysis is restricted to the inviscid flow.

An application of SCM to multistage steam turbines was made by Renaudin and Somm (14). The method uses the blade height for a given mass flow as the boundary condition instead of the mass flow for a given blade height more

commonly used. Streamlines have been assumed to be elastic lines which are a function of time instead of space used in similar spline fitting techniques.

Katsanis (4) has used the method in conjunction with the Matrix method for evaluation of transonic flows which is not possible using the Matrix method. Silvester and Hetherington (15) have also developed the method independently on the same lines as that of Novak (9).

In an application to gas turbine design, Carter, Platt and Lenherr (16) have used the SCM for the evaluation of the design point performance of axial turbines and also as a tool to evaluate different designs during the design stage of the turbines. The radial equilibrium equation has been simplified by neglecting the term involving the change in momentum in the meridional direction by assuming that the streamline slopes are small. The slope and curvature of the streamlines were evaluated from the slopes and curvatures of the hub and casing boundaries by assuming a linear variation from the hub to casing for them. This is in contrast to the "spline-fitting" technique adopted by Novak (9), Jansen and Moffat (10), Silvester and Hetherington (15), among others. A loss correlation has also been developed by evaluating the pressure loss coefficients from the blade angles of the blade row and correlating them with

the efficiency plots of Smith (17). Effect of interfilament mixing and coolant injection has also been included in the computer program.

1.1.4 Comparison of the Matrix and Streamline Curvature Methods

A comparison of the matrix method and the streamline curvature method has been made by Davis and Millar (18). One of the important conclusions drawn by them is that it is not possible for either method to claim a clear operational advantage over the other. Some of the advantages claimed for the matrix method are slightly better accuracy and stability of the computing procedure. However the matrix method requires a large computer storage for implementation. Some of the advantages of the streamline curvature method are its ability to handle transonic flows and small computer storage for implementation. Another important conclusion drawn by Davis and Millar has been that the accuracy with which the flow is predicted is ultimately dependent on the cascade model used for the evaluation of losses in a blade row.

The ability to handle transonic flows is an important requirement for axial turbine analysis as the flow at the first stator exit is invariably transonic. Along with this, the need for only small computer storage requirement led to the choice of the streamline curvature method in the present work.

1.2 Loss model

The equations of flow used in the methods discussed, above, are for an inviscid flow. However, the analysis of the inviscid flow would be of little use in the prediction of performance of the turbomachine unless some method is found to take into account the changes in entropy due to viscosity. This is the purpose of the loss model. The loss model superposes on the inviscid flow the effects of viscosity in the form of losses occuring in the flow. These losses may be superposed in the form of a stagnation pressure loss, an increase in entropy, loss in kinetic energy, or by the use of efficiencies.

The evaluation of the losses in the flow is usually achieved from correlations of experimental data. A large amount of such data is available in the case of axial compressors. A NASA special publication (NASA SP-36) on axial compressors contains a collection of such data. Mazumdar (19) has reviewed the different correlations available for axial compressors. In the case of axial turbines, however, loss correlations are limited. Two of the wellknown and much used correlations are the Ainley-Mathieson correlation and the Soderberg correlation (Horlock (20)).

Another method of evaluating the losses in the flow is by solving the boundary layer equations. This is the

current trend in turbomachine calculations. The end-wall boundary layers are three-dimensional and the solution of the three-dimensional boundary layer equations is too complex for implementation into a design-analysis computing system.

While the evaluation of losses is in itself important, the distribution of these losses along the blade height has also to be taken into account. The distribution of these losses must be determined from experimental data. Unfortunately, such data is not available in published literature. The radial distribution of these losses, therefore, should be made in a simplified manner consistent with the nature of the flow. Jansen (21) has made such an attempt for centrifugal compressors. The skin friction losses have been distributed in proportion to the wetted area and square of the velocity. The clearance losses have been distributed between the first four streamtubes, at the blade tip, in a specified proportion. Results obtained however have not been compared against experimental data.

1.3 Scope of present investigations

The streamline curvature method is a well established method for turbomachine flow analysis which can be implemented on a relatively small computer system. This along with the fact that the method can be used for transonic flows led to its choice in this work for the design-point performance

prediction of axial turbines.

The accuracy with which the performance can be predicted depends to a large extent on the loss model used. As already explained, it is also necessary that these losses be distributed appropriately along the blade height. A loss model using well known loss correlations but also taking into account the distribution of these losses has sought to be developed here.

CHAPTER 2

FORMULATION AND APPROACH TO SOLUTION

2.1 Formulation

The inviscid three-dimensional flow pattern can be found by solving the following equations

(1)	Continuity	(1 equation)
(2)	Motion	(3 equations)
(3)	Energy	(1 equation)
(4)	State	(1 equation)

Solution of these six equations determine the fluid properties ρ, h and s and the three velocity components V_r, V_u and V_x. For a reversible adiabatic flow the three equations of motion can be combined with the energy equation to obtain an equation that states that the entropy of the fluid remains constant along any streamline. Since the equations of motion, energy and entropy are interdependent, solutions can be obtained by using any four of them, the fifth being automatically satisfied.

If the reversible adiabatic flow takes place on a prescribed stream surface (the meridional surface), then there exists a geometrical condition relating the three components of the velocity vector in order that the velocity vector lies in the stream surface.

With this sixth equation, there is a redundancy of one equation and the flow pattern is obtained by replacing one of the equations of motion with the geometrical condition for the flow to remain in the stream surface. The replaced equation of motion can be used to evaluate the force necessary to keep the flow in the stream surface. This force, for an inviscid flow, lies normal to the surface and is contained only in the equation of motion for this direction. Thus this equation is replaced by the geometrical condition for the flow to remain in the stream surface and can be used to evaluate the force required to do so.

Thus for a reversible adiabatic flow on a prescribed stream surface the flow pattern can be determined by the following six equations

(1) Continuity

(2)(a) Any two of : X equation of motion
r equation of motion
Entropy

(b) Geometrical condition

(3) Energy

(4) State

For an irreversible adiabatic flow, the entropy increases along the streamline and this effect is taken into account by means of the loss model. Since the irreversibility

of the flow is caused by viscous effects, the introduction of a loss model superposes the viscous effects of the real flow on an otherwise inviscid formulation. This leads to a certain inconsistency in the equations (Horlock (22))as the equations are basically for an inviscid flow. An alternate formulation to avoid this inconsistency, proposed by Horlock (22) and also used by Bosman and Marsh (5) has been shown to be invalid by Wu (23). Also, in spite of this inconsistency, the numerical solutions for the flow pattern by using loss models - have been very successful in meridional flow predictions. It is this set of equations that are widely used in the analysis of the flow in turbomachines and has been used in the present investigation.

Thus, for an irreversible adiabatic flow on a prescribed stream surface, the six governing equations are :

1) Continuity
2) a) Motion (r direction)
   b) Entropy (loss model)
   c) Geometrical condition
3) Energy
4) State.

The equation of motion in the r direction describes the equilibrium of the flow along the radius and is the well known radial equilibrium equation.

2.2 The equations

2.2.1 Radial equilibrium equation

In the derivation of the radial equilibrium equation the following assumptions have been made.

1. The flow in inviscid.
2. The rotor is rigid and rotates with constant angular velocity
3. The fluid is a semiperfect gas i.e. the equation of state is $P = \rho RT$ (2.1)
   with R constant, and the specific heats are dependent upon the temperature only.
4. The flow is steady and axisymmetric.

For a frame of reference rotating with constant angular velocity ω about the x axis, Newton's second law of motion gives for an inviscid fluid, (Figure (2))

$$-\frac{\nabla p}{\rho} = \frac{D\vec{W}}{Dt} - \omega^2\vec{r} + 2\vec{\omega} \times \vec{W} \qquad (2.2)$$

The unit vector derivatives are

$$\frac{D\vec{i}_r}{Dt} = \frac{W_u}{r}\vec{i}_u \text{ and } \frac{D\vec{i}_u}{Dt} = -\frac{W_u}{r}\vec{i}_r$$

and the kinematic relation $\frac{D(\ )}{Dt} = W\frac{D(\ )}{Ds}$.

The "D" -operator signifies that a fluid particle is being followed during differentiation. The equation (2.2)

can be written in terms of its scalar components as.

$$-\frac{1}{\rho}\frac{\partial p}{\partial r} = W\frac{DW_r}{Ds} - \frac{(W_u + \omega r)^2}{r} \tag{2.2a}$$

$$-\frac{1}{\rho}\frac{\partial p}{r\partial\theta} = W\frac{DW_u}{Ds} + \frac{W_u W_r}{r} + 2\omega W_r \tag{2.3b}$$

$$-\frac{1}{\rho}\frac{\partial p}{\partial x} = W\frac{DW_x}{Ds} \tag{2.3c}$$

Using the substitution $V_u = W_u + \omega r$ between the absolute and relative velocities, equations (2.3a) and (2.3b) can be rewritten as.

$$-\frac{1}{\rho}\frac{\partial p}{\partial r} = W\frac{DW_r}{Ds} - \frac{V_u^2}{r} \tag{2.4a}$$

$$-\frac{1}{\rho}\frac{1}{r}\frac{\partial p}{\partial\theta} = \frac{W}{r}\frac{D}{Ds}(r V_u) \tag{2.4b}$$

We can also write,

$$W\frac{D(\ )}{Ds} = W_x\frac{D(\ )}{Dx} \tag{2.5}$$

where Dx represents the increase in the x coordinate the particle undergoes as it moves a distance Ds in the flow direction. Equations like (2.5) can be written for any desired direction. Written for the meridional direction, defined by

$$\vec{i}_m\, Dm = \vec{i}_x\, Dx + \vec{i}_r\, Dr \tag{2.6}$$

equation (2.5) becomes

$$W\frac{D(\ )}{Ds} = W_m\frac{D(\ )}{Dm} \tag{2.7}$$

Substituting equation (2.7) in equation (2.4a), we get,

$$-\frac{1}{\rho}\frac{\partial p}{\partial r} = W_m \frac{DW_r}{Dm} - \frac{V_u^2}{r} \tag{2.8}$$

Further, we can write $W_r = W_m \sin\phi$ (2.9)

and equation (2.8) can be rewritten as

$$\frac{1}{\rho}\frac{\partial p}{\partial r} = \frac{V_u^2}{r} - V_m^2 \frac{D \sin\phi}{Dm} - W_m \sin\phi \frac{DW_m}{Dm} \tag{2.10}$$

Now, $$\frac{D \sin\phi}{Dm} = \cos\phi \frac{D\phi}{Dm}$$

and $$\frac{D\phi}{Dm} = -\frac{1}{r_m} \tag{2.11}$$

The radius of curvature is considered negative when the streamline projection on the meridional plane is concave upward.

Equation (2.10) can now be rewritten as

$$\frac{1}{\rho}\frac{\partial p}{\partial r} = \frac{V_u^2}{r} + \cos\phi \frac{W_m^2}{r_m} - W_r \frac{DW_m}{Dm} \tag{2.12}$$

Written in terms of the absolute velocity components, equation (2.12) becomes

$$\frac{1}{\rho}\frac{\partial p}{\partial r} = \frac{V_u^2}{r} + \cos\phi \frac{V_m^2}{r_m} - V_m \sin\phi \frac{DV_m}{Dr} \tag{2.13}$$

Equation (2.13) is written in a more convenient form by replacing the static pressure by the stagnation pressure from

$$p = p_o \left[1 - \frac{V_u^2 + V_m^2}{2c_p T_o}\right]^{\gamma/\gamma-1}$$

We get

$$\frac{V_u^2+V_m^2}{2}\ \frac{1}{T_o}\frac{dT_o}{dr} - V_u\frac{dV_u}{dr} - \frac{1}{2}\frac{dV_m^2}{dr} + R\,T_o\left[1 - \frac{V_u^2+V_m^2}{2c_pT_o}\right]\frac{1}{\rho_o}\frac{dp_o}{dr} =$$

$$\frac{V_u^2}{r} + \frac{V_m^2}{r_m}\cos\phi - V_m\sin\phi\ \frac{DV_m}{Dm} \qquad (2.14)$$

It is now necessary to express the term $\frac{DV_m}{Dm}$ in terms of the meridional pathline slope and curvature. By making use of the continuity equation, equation of state, and laws of thermodynamics, it can be shown that (Appendix A)

$$\sin\phi\ \frac{DV_m}{Dm} = \frac{V_m\left[\left(1 + M_\theta^2 + \frac{r}{r_m\cos\phi}\right)\frac{\sin^2\phi}{r} + \tan\phi\ \frac{\partial\phi}{\partial r}\right]}{1 - M_m^2} \qquad (2.15)$$

Smith (8) has derived the above equations by defining averages of the flow properties in the circumferential direction. It has also been shown that the equations are the same as that derived by Novak (9) by making the axisymmetric approximation when the "G-functions" defined by Smith (8) can be neglected. It is evident from the analysis of Smith (8) that the evaluation of the G-functions is too difficult to be incorporated in a meridional flow solution method. Another difference between the approaches of Smith (8) and Novak (9) is in the choice of the dependent variable in the radial equilibrium equation. While Smith has used the static pressure, Novak has used the meridional velocity as the primary dependent variable. This

is purely a matter of convenience and the meridional velocity, as adopted by Novak (9), has been used here as the dependent variable.

2.2.2 The Continuity Equation

The continuity equation provides the necessary condition for the determination of the constant of integration when integrating the radial equilibrium equation. In other words it provides the necessary boundary condition for the radial equilibrium equation. Thus while the radial equilibrium equation determines the distribution of the meridional velocity across the annulus, the continuity equation determines the magnitude of these velocities so as to satisfy design mass flow specifications.

For an axisymmetric flow passing through an axial section of an arbitrary annulus, the continuity equation can be written in its integral form as

$$W_T = 2\pi \int_{r_h}^{r_t} \rho \, V_x \, r \, dr \qquad (2.16)$$

The equation is written in a more convenient form in terms of the total temperature, total pressure and the tangential and meridional components of the absolute velocity which have been chosen as the principal variables in the analysis. The density can be written in terms of the total pressure and total temperature as

$$\rho = \frac{p_o}{RT_o}\left[1 - \frac{V^2}{2c_pT_o}\right]^{\frac{1}{\gamma-1}} \qquad (2.17)$$

Substitute (2.17) in (2.16) to get

$$w_T = \frac{2\pi}{R}\int_{r_h}^{r_t} \frac{p_o}{T_o}\left[1 - \frac{V_u^2 + V_m^2}{2c_pT_o}\right]^{\frac{1}{\gamma-1}} V_m \cos\phi \; r \, dr \qquad (2.18)$$

2.2.3 The loss equation

Since the total temperature and total pressure are chosen as the principal variables in the analysis, the irreversibility of the flow is more conveniently expressed in terms of a stagnation pressure loss than in terms of the increase in entropy. For this purpose a total-pressure-loss coefficient is defined as follows :

$$Y_N = \frac{p_{oo} - p_{o1}}{p_{o1} - p_1} \qquad (2.19)$$

or
$$p_{o1} = \frac{p_{oo}}{1 + Y_N\left(1 - \frac{p_1}{p_{o1}}\right)} \qquad (2.20)$$

For a rotor, the loss coefficient is defined as (Figure 3)

$$Y_R = \frac{p'_{o2s} - p'_{o2}}{p'_{o2} - p_2} \qquad (2.21)$$

or
$$p'_{o2} = \frac{p'_{o2s}}{1 + Y_R\left(1 - \frac{p_2}{p'_{o2}}\right)} \qquad (2.22)$$

The above equations can be used to determine the stagnation pressure loss when the total-pressure-loss coefficient is known.

The loss coefficient is evaluated from the correlations of experimental loss data in the form of a loss model.

If the option of specifying stage isentropic or rotor isentropic efficiencies is used, equations similar to (2.20) and (2.22) can be written for the stage outlet stagnation pressure

$$p_{o2} = p_{oo}\left[1 - \frac{T_{o1} - T_{o2}}{\eta_s T_{oo}}\right]^{\frac{\gamma}{\gamma-1}} \tag{2.23}$$

$$p_{o2} = p_{o1}\left[1 - \frac{T_{o1} - T_{o2}}{\eta_R T_{oo}}\right]^{\frac{\gamma}{\gamma-1}} \tag{2.24}$$

2.2.5 The work equation

The necessary equation relating the tangential velocity to other principal variables is provided, at a rotor exit, by the Euler work equation.

$$c_p \Delta T_o = V_{u1} u_1 - V_{u2} u_2 \tag{2.25}$$

or
$$V_{u2} = \frac{V_{u1} u_1 - c_p \Delta T_o}{u_2} \tag{2.26}$$

This equation is used in the analysis when the design work is specified.

2.2.6 Geometrical conditions

At a stator exit the tangential velocity is related to the meridional velocity from a specification of the exit flow angle in the velocity triangle.

$$V_u = V_m \cos \phi \tan \beta \qquad (2.27)$$

When the complete velocity triangles are specified, the tangential velocity at a rotor exit can be related to the meridional velocity by an equation similar to (2.27). This equation replaces the Euler work equation for the tangential velocity in the analysis of the flow. The Euler work equation (2.25) can now be used for the evaluation of the total temperature drop through a stage and hence the total temperature at the stage exit.

2.3 Approach to the solution of the equations.

The solution of the flow field in a turbine consists essentially of obtaining values of the total pressure, total temperature, and the two components of the absolute velocity at each selected streamline location in each of the radial planes at which the solution is being obtained (design plane). Thus, for the analysis p_o, T_o, V_u, and V_m are the principal variables. In the previous section all the equations which have to be satisfied in the analysis have been presented in terms of these variables. The technique for solution adopted here is similar to that by Carter, et. al. (16).

The set of equations, for the solution, would comprise of equation (2.14), the appropriate equation in the set of equations (2.19) to (2.24), equation (2.25) or (2.26) and equation (2.27). It is obvious that the principal equation in

this set is the radial equilibrium equation (2.14). This equation is an ordinary differential equation, nonlinear in the variable V_m. The remaining of the equations can now be used for the evaluation of the other flow variables in equation (2.14). The total temperature is evaluated from the Euler work equation (2.25). (Appendix B). In addition, the streamline slope and curvature in the meridional plane necessitates consideration of derivatives with respect to the axial direction x. That is :

$$\phi = \tan^{-1} \left(\frac{dr}{dx}\right) \tag{2.28}$$

$$\frac{1}{r_m} = \frac{d^2r/dx^2}{\left[1 + (dr/dx)^2\right]^{3/2}} \tag{2.29}$$

Hence, the radial equilibrium equation (2.14) contains derivatives with respect to both r and x. It is unrealistic to assume that the axisymmetric form of the radial equilibrium equation can be extended beyond the interblade row space into the blade rows. Thus, the boundary conditions for the meridional streamlines in the interblade row space are indeterminate at the trailing edge and leading edge planes, defining this space. Only the boundary streamlines, at the inner and outer walls, are defined by the assumption that these streamlines follow the contours of the annulus wall. In the absence of a rigorous analytical treatment for the slope and curvature of the streamlines in the meridional plane, it

becomes necessary to make more assumptions for the solution of the problem. In the present analysis, the streamline slope and curvature in the meridional plane has been calculated in one of two ways.

a) The slope and curvature of the boundary streamlines be obtained from a definition of the wall contours, and then both ϕ and r_m will be assumed to be linear functions of radius determined from the values at the walls.

b) The use of spline-fitting techniques.

Detailed discussion on these methods is presented in a later chapter.

A numerical solution of the equation (2.14), clearly, has to be iterative. The continuity equation (2.16) provides the necessary boundary condition for the evaluation of the constant of integration in equation (2.14).

2.4 The differential equations

In presenting the equations here, the case of a single stage turbine has been considered with design stations at the stator inlet, stator exit, and the stage exit. A multistage turbine can be considered as merely repeating the solution technique of the first stator exit and the first stage exit planes.

The radial equilibrium equation (2.14) can be written

in the form

$$C_{11} \frac{dV_m^2}{dr} + C_{12} \frac{1}{p_o} \frac{dp_o}{dr} + C_{13} \frac{dV_u}{dr} = C_{14} \qquad (2.30)$$

where the coefficient C_{11}, C_{12}, C_{13} and C_{14} can be assigned values at each point in a particular design plane once a value of meridional velocity is selected. The variables T_o, ϕ, r_m and r and constants γ and c_p are assumed to have been evaluated.

The differentiation of the appropriate equation for total pressure (Any of the equations (2.20), (2.22), (2.23) or (2.24), depending on the station and option being considered) leads to a differential equation also of the form

$$C_{21} \frac{dV_m^2}{dr} + C_{22} \frac{1}{p_o} \frac{dp_o}{dr} + C_{23} \frac{dV_u}{dr} = C_{24} \qquad (2.31)$$

where the coefficients C_{21}, C_{22}, C_{23} and C_{24} can be evaluated in terms of the input specifications and meridional velocity.

Similarly, differentiation of either of the equations (2.26) or (2.27) for V_u results in a differential equation again of the form

$$C_{31} \frac{dV_m^2}{dr} + C_{32} \frac{1}{p_o} \frac{dp_o}{dr} + C_{33} \frac{dV_u}{dr} = C_{34} \qquad (2.32)$$

In this case coefficient C_{32} is always zero.

The terms involved in the coefficients are presented in Appendix (C) after differentiation of appropriate equations.

2.5 Technique for solution

The rewriting of the equations of Chapter 2 in the form (2.30), (2.31) and (2.32) helps in developing an unique technique for the solution irrespective of the design station being considered, only the coefficients of the differential equation differ from station to station. The problem of solution is now one of obtaining a meridional velocity distribution which simultaneously satisfies the radial equilibrium and continuity equations. By choosing an initial value of the meridional velocity at one streamline position, the local values of the coefficients of the set of equations (2.30), (2.31) and (2.32) can be obtained. These equations are now solved for the derivative dV_m^2/dr. Using the standard Runge-Kutta-Gill method of solving ordinary differential equations (Appendix D), the value of the meridional velocity at an adjacent streamline can be obtained. Using the new value of the meridional velocity, values of the total pressure, tangential velocity, and the coefficients can be obtained at the new streamline. Thus the derivative dV_m^2/dr can be obtained at this new streamline also. The process is repeated until the meridional velocity, total pressure, and tangential velocity are obtained at each of the streamlines used in the analysis. Using the continuity equation (2.18), the mass flow for the meridional velocity distribution obtained is

evaluated. Since the solution was obtained from an assumed value of the meridional velocity at one point in the flow field, the mass flow computed will in general differ from the design specified value. Hence, the assumed value of the meridional velocity will have to be modified iteratively until the starting value is consistent with the continuity requirement. This constitutes the inner loop of the iteration procedure at a design station.

The outer loop of the iteration scheme is dependent on the method adopted for evaluating the streamline slope and curvature. First, we assume that method (a) of section 2.3, above, is chosen for this purpose. In this case, it is clear that the slopes and curvatures are functions of only radius at a given design station. It is now possible to complete the outer loop of the iteration scheme at the design station before proceeding to the next station downstream. This is completed as follows :- Since initially the flow distribution is unknown, the initial streamline positions are estimated from equal areas for each stream tube. Hence, streamline positions have to be relocated after each solution of the radial equilibrium and continuity equations until a converged solution for streamline positions has been obtained. This completes the solution at a design station and the analysis can proceed to the next design station downstream.

In the case of adopting the method of spline fitting, method (b) of section 2.3, a new iteration scheme has to be applied for the outer loop. The reason for this is that in spline fitting, the slopes and curvatures are functions of the radial position of streamlines at upstream and downstream stations also. Thus it is necessary to complete the inner iteration loop at all design stations in the turbine annulus, the streamlines be relocated at these stations as in the previous methods, and a new set of spline curves be fitted in the annulus. Thus, after completing the inner loop at a design station, the analysis proceeds to the next design station downstream till the entire turbine annulus is traversed. Streamlines are relocated at all the design stations and spline curves are fitted to simulate a new set of streamlines. The inner loop is again started at the first station and proceeds downstream till the annulus is traversed. This process is repeated till convergence of streamline positions is obtained.

CHAPTER 3

LOSS MODEL

3.1 Introduction

The task of predicting the design-point performance of of an axial turbine can be accomplished only when the viscous effects of the flow can be incorporated into the basically inviscid calculation of the streamline-curvature method. This, as has been explained in Chapter 3, is achieved by replacing one of the momentum equations by an equation which describes the loss of stagnation pressure in a blade row. In using this equation (eqns. 2.19 or 2.23), it is clear that the pressure-loss-coefficient, Y, or the blade row efficiency, η, should be known beforehand. This, then is the purpose of the loss model.

It is self-evident at this stage that even though the preparation of numerical procedures for the streamline-curvature method of performance prediction is of importance in itself, unless the procedure incorporates soundly based assumptions concerning the losses associated with the elements of the blading, the detailed calculations of interblade row aerodynamics will be of little value. Hence, an essential part of the development of a design analysis computing system is the development of a loss correlation which would be an integral part of the computer program.

Unlike the case of axial compressors, loss data is limited in the case of axial turbines. Two of the most commonly used correlations are the Soderberg correlation and the Ainley-Mathieson correlation. These correlations have been developed using data obtained from steam turbines and early gas turbines. However, these correlations are still in use in modified forms because of lack of other reliable data (Horlock (20)).

Three loss models have been used in this work. Two of these have been developed by Carter, et. al. (16) and the third has been developed here to rectify some important drawbacks of the other two models. These loss models have been described in detail in next section of the chapter.

3.3.1 Loss model - 1

This is the simplest of the loss models wherein loss data in the form of pressure-loss-coefficients, kinetic-energy loss coefficients or blade efficiencies are specified in the input data to the computer program. Evidently, such a model can be used only when data is available from experimental investigations on the turbine being analysed or from experience obtained from other similar turbine investigations. The use of such a loss model is restrictive and may be used in preliminary design analyses.

3.3.2 Loss model - 2

The loss correlation used in this model has been developed by Carter, et. al. (16). The detailed development of the correlation is available in that reference. The starting point of this development is the Soderberg correlation given below.

$$Y = (0.00078 + 0.00000582^2)\ \{3-9(V_{in}/V_{ex})+10(V_{in}/V_{ex})^2\} \qquad \ldots(3.1)$$

The above correlation implies that when the velocity ratio, V_{in}/V_{ex}, falls below 0.45, the level of loss for a given deflection begins to increase. This is contradictory to the expectation that the losses would decrease smoothly as the over-all row acceleration increases at a constant deflection. To overcome this discrepancy, Carter, et. al. (16) have assumed that the losses are proportional to the blade inlet and exit angles instead of on the deflection as in the Soderberg correlation. They have developed a correlation of the form.

$$Y = \frac{|\tan\beta_{in} - \tan\beta_{ex}|}{(a_4 + a_4\cos\beta_{ex})}\ \{a_1+a_2(V_{in}/V_{ex} - a_3)\}$$

$$\text{if } V_{in}/V_{ex} \geq a_3 \qquad (3.2a)$$

$$\text{and}\quad Y = \frac{|\tan\beta_{in} - \tan\beta_{ex}|}{(a_4 + a_5\cos\beta_{ex})}\ \{a_6 + a_7(V_{in}/V_{ex})^{a_8}\}$$

$$\text{if } V_{in}/V_{ex} < a_3 \qquad (3.2b)$$

The basis of the correlation are the efficiency plots of Smith (17). Carter, et. al. (16) have assumed that the efficiencies obtained from this plot are the achievable efficiencies of the design being analysed. With this assumption, the constants a_1 to a_9 in the correlation have been evaluated so that it predicts the efficiencies of Smiths (17) plot.

3.3.3 Loss model 3

The loss model described here has been developed to overcome some important shortcomings of the two other loss models just described. As explained earlier, the use of the first loss model is limited by the availability of data to use blade row efficiencies as inputs to the calculation scheme. A scrutiny of the development of the second loss model shows that the loss levels calculated from the correlation are primarily dependent on the blade angles of the blade row. Thus, the distribution of losses across the annulus would reflect the trend in the distribution of the blade angles. As an example, if the blade angles are largest at the hub and least at the tip, as is true in many turbines, the loss levels calculated using correlation (3.2) would show minimum losses at the tip and maximum losses at the hub. This distribution is contrary to experimental observations and qualitative studies based on the nature of losses in a blade row which show that the losses are minimum around the

centre of the annulus and increase towards the hub and tip (24, 25, 26). Thus, while the correlation (3.2) may predict the overall efficiencies and average loss levels accurately, it cannot predict the distribution of these losses across the annulus.

To analyse the distribution of losses in the annulus of a turbine, it is essential to seperate the losses into its principal constituents, namely, the profile loss and the secondary loss. The profile loss caused by the boundary layer on the suction and pressure surfaces of the blade is dependent on the blade angles (Horlock (20), Balje (25)). Thus, it would be reasonable to assume that the profile loss calculated from correlations based on blade angles would reflect the correct trend of profile loss distribution in the turbine annulus. The secondary losses are caused by the three-dimensional boundary layer at the hub and tip of the turbine annulus. While it may be possible to calculate the overall level of secondary loss from correlations based on blade angles, their distribution in the turbine annulus cannot be obtained from such a correlation. Qualitative explanations and measurements (Hanley (24), Balje (25), Hosney (26)) show that the secondary losses are maximum in the hub and tip regions and negligible in the centre of the annulus.

Therefore in the development of a loss model, it is essential to calculate the profile and secondary losses separately and to take into account the difference in their distributions in the turbine annulus. In the present loss model, the profile loss has been calculated using the well known Ainley-Mathieson correlation (Horlock (20))

$$Y_p = \left[Y_{p(\beta_1=0)} + \left(\frac{\alpha_1}{\alpha_2}\right)^2 \left(Y_{p(\beta_1=\beta_2)} - Y_{p(\beta_1=0)}\right)\right] \left(\frac{b_t/b_c}{0.20}\right)^{\beta_1/\beta_2} \qquad (3.3)$$

The losses are evaluated at each streamline in the calculation scheme and since the correlation is primarily dependent on the blade angles, the distribution of the profile loss would be accurate.

Many correlations are available for the evaluation of secondary losses (Dunham and Came (27)). In their review, Dunham and Came (27) have concluded that the best correlation is of the form.

$$Y_s = b_c/b_h(\cos\beta_2/\cos\beta_1)(C_l/b_s/b_c)^2 \cos^2\beta_2/\cos^3\beta_m \text{ function } (\delta_1/b_c) \qquad (3.4)$$

The evaluation of the inlet boundary layer thickness, δ_1, is difficult in the present calculation scheme and the function

is assumed to be constant. Dunham and Came (28) have used a value of 0.0334 for this constant.

$$Y_s = 0.0334 \left(\frac{b}{b_n}\right) \left(\frac{\cos \beta_2}{\cos \beta_1}\right) Z \tag{3.5}$$

where Z is the Ainley-Mathieson loading parameter

$$Z = \left(\frac{C_\ell}{b_s/b_c}\right)^2 \frac{\cos^2 \beta_2}{\cos^3 \beta_m} \tag{3.6}$$

The secondary losses were distributed across the annulus in a parabolic form.

$$Y_s(r) = A\, r^2 + Br + C \tag{3.7}$$

The evaluation of A, B, and C requires three conditions which have been assumed taking into consideration the nature of distribution of the secondary loss in the turbine annulus.

(1) The mass-averaged secondary loss obtained from (3.7) is that evaluated using the correlation (3.5)

(2) The secondary losses are zero at the mean streamline.

(3) The slope of the distribution is zero at the mean streamline.

The three conditions determine the values of A, B and C in (3.7) and the expression can be used to evaluate the secondary loss at any streamline in the annulus. Thus, the total loss at any streamline is,

$$Y = Y_p + Y_s(r).$$

CHAPTER 4

COMPUTER PROGRAM

4.1 General Description of the Computer Program

The basic equations which govern the design point performance of an axial flow turbine and the method of their solution has been presented in previous chapters. The numerical method of solution is best implemented on a digital computer. The computer program for this purpose, used here, has been based on the computer program of Carter et. al. (29). A general description of the program is given below.

The program has been written in Fortran IV for use on an IBM 7044/1401 data processing system. It is capable of analysing both single and multispool units (a maximum of three spools is allowed) and each spool may have upto eight stages. The absolute and relative flow fields are computed at the first stator inlet, at each interblade row plane, and at the final rotor exit. The effects of blade coolant flows, interfilament mixing and a station-to-station variation of the specific heat can be included. The loss correlations described in Chapter 3 have been incorporated into the program and any one of them can be used by changing an index on the program coding card in the input data. Options are also available for use of both the methods of calculation

of streamline slope and curvature mentioned in Chapter 2, the option being exercised, again, by change of an index in the coding card. Iteration schemes are suitably modified by this change of index and no further changes in the program are necessary. It is also possible to feed the streamline slopes and curvatures as input data into the program.

A number of options are available for the input data required by the program depending on the nature of the data available. These have been described below along with the data required.

The general specification of the turbine consists of :

1. Number of spools.
2. Gas constant of the working fluid.
3. Mass flow at the turbine inlet.
4. Flow conditions at the inlet of the turbine (total temperature, total pressure, and flow angle as a function of radius).

The spool specification consists of

1. Rotative speed.
2. Power output if rotor exit relative angles are not specified.

Finally, the spool analysis variables consist of :

1. Number of stages.
2. Power output of each stage if rotor exit relative angles are not specified.

3. Specific heat at spool inlet and each blade row exit station.
4. Annulus geometry and axial position of each station.
5. Mass flow and total temperature of the coolant added if the turbine is cooled.
6. Streamline values of the mixing coefficient for each blade row if interfilament mixing is specified.
7. Whirl velocity or flow angle as a function of radius at each stator exit.
8. Streamline values of the power output distribution or the rotor relative exit angles.
9. Stage efficiency, rotor efficiency, total-pressure-loss coefficient, or kinetic-energy - loss coefficient, and additional loss factors when desired, when the losses are not calculated from the loss correlation available in the program.

The output of the program consists entirely of printed data. The information included in the output can be listed as follows :

1. All input data.
2. Tabulated streamline values of the flow parameters obtained from the converged solution.
3. Tabulated streamline values of the mixed and/or cooled flow parameters for a blade row.
4. Tabulated streamline values of the performance parameters of the stator and rotor blade rows.

5. Mass averaged performance parameters for a stage.
6. Tabulated mass averaged performance parameters for each stage of a spool.
7. Mass averaged performance parameters for a spool.
8. Mass averaged performance parameters for the turbine.
9. In addition streamline values of the flow parameters through each iteration of the computation can also be printed if desired.

Some inbuilt checks have been incorporated into the program to continuously monitor the computational process. The purpose is to abandon the calculation when it is clear that a converged solution may not be possible and continuation of the computation is not worthwhile. Such cases occur due to numerical instability and oscillation of the solution. For example, when the design mass flow is close to or greater than the choking mass flow at the station may lead to oscillations in the inner iteration loop with no convergence of the mass flow. Other cases may be when it is not possible to satisfy radial equilibrium and the continuity equations simultaneously, oscillations in the outer iteration loop, and so on. In all cases streamline values of the flow parameters at the last iteration are printed along with a message explaining the reason for abandoning the computation. Nine such messages are incorporated in the program and cover possible problems that may occur in the computation.

4.2 Interfilament Mixing

The presence of large gradients of the flow properties in the flow field would result in flow mixing that would try to reduce these gradients. To integrate the effects of mixing into the computer program, a simple flow model has been used by Carter et. al. (16) which has been retained in this work. No attempt has been made to represent the complex processes by which mixing takes place but to qualitatively represent the mass flow mixing which occurs between the stream filaments.

The consideration that if a total pressure and total temperature profile is modified by mixing, the new profile would have the original mass flow weighted values leads to the formulation of a mixing model of the form :

$$p^*_{oj} = (1 - \mu_j)\, p_{oj} + \mu_j \frac{\sum_k \mu_k \Delta w_k p_{ok}}{\sum_k \mu_k \Delta w_k} \qquad (4.1a)$$

$$T^*_{oj} = (1 - \mu_j)\, T_{oj} + \mu_j \frac{\sum_k \mu_k \Delta w_k T_{ok}}{\sum_k \mu_k \Delta w_k} \qquad (4.1b)$$

The mixing parameter, μ_j, is specified for individual streamlines in the input data, but the same value is used for both total pressure and total temperature.

Having chosen a mathematical formulation for mixing, it is necessary to decide at what point it is to be introduced into the analysis. Since mixing is related to the flow within a blade row, it would appear logical to specify mixing

parameters for blade rows rather than calculation stations. The modification from streamline to mixed values of absolute total pressure and total temperature are made downstream of the plane at which radial equilibrium and continuity equations are satisfied and the mixed values are used in the inlet conditions for the following blade row in which mixing is assumed to occur.

4.3 Modifications to the Computer Program of Ref. (29)

During the initial use of the computer program, it was found necessary to modify certain parts of the computer program of Carter et. al. (29). These modifications are discussed below.

4.3.1. Improvements when choking flow conditions are encountered

Use of the basic computer program of Carter, et.al. (29) at stations where choking flow occured (usually the first stator exit) resulted in oscillations of the solution and consequent abandoning of the calculation. Closer scrutiny showed that the reason for these oscillations was too large a change in the meridional velocity from one iteration to the next of the inner loop. This resulted in the mass flow oscillating about the choking mass flow without convergence. The obvious solution to the problem was to use damping techniques on the meridional velocity

$$V_m^{(2)} = \lambda\, V_m^{(1)} + (1 - \lambda)\, V_{m1}^{(2)} \qquad (4.2)$$

where $V_{m1}^{(2)}$ is the value of the meridional velocity calculated for the new iteration, $V_m^{(1)}$ the value for the previous iteration, and $V_m^{(2)}$ the value used in the new iteration which is the damped value. A value of λ between 0.7 and 0.8 was found necessary to effectively damp the oscillations. It must be emphasised that damping is used in the program only when oscillations are sensed by it. In other circumstances the value $V_{m1}^{(2)}$ is used with no damping and thus quicker convergence to the specified mass flow.

4.3.2 The use of rotor relative exit angles instead of work specification

The use of the program when the work done by the turbine is specified requires also the specification of the distribution of the work across the blade height. In other words, the loading of each section of the blade has to be specified. This was found to be inconvenient because rarely is the exact loading pattern known for a performance evaluation. However, the velocity triangles of the turbine are usually known and the rotor relative exit angles provide a better input into the program. The equation (2.27) replaces the equation (2.26) in the analysis and the stagnation temperature drop across the rotor is calculated from equation (2.25).

The use of either the work done or the rotor relative exit angle as an input is an option available to the user and

the option is easily exercised by a change in index in the initial coding card of the input data. The work specification can be used for turbine design and the exit angle specification for the design-analysis.

4.3.3 The use of spline fitting techniques to evaluate streamline slope and curvatures

The use of spline fitting techniques have been adopted by most authors for calculating the streamline slope and curvature (Novak (9), Frost (12), Silvester and Hetherington (15), among others). The method has been incorporated in the present computer program.

Daneshywar, et. al. (30) has made a critical assessment of this method for use in the streamline curvature technique. The conclusion is that the instability that may incur in the method is due to oscillations of the second derivative of the spline curve which is used to calculate the streamline curvature. To overcome this problem, Daneshywar (30) has suggested the use of two spline curves, the first one fitted to points through which the streamline passes, from which the streamline slopes are calculated, the second one fitted to the calculated slopes at the given axial stations and is used to calculate the second derivative and hence the streamline curvature. The method, called the 'Double-Spline Fit', is described in detail below.

The radial points through which the streamline is to pass along with their axial positions form a set of data points which is denoted by (x_1,r_1), (x_2,r_2) ... (x_N, r_N). A spline curve is made to pass through this set of data points and this curve can be defined analytically in the interval $\ell_k = x_k - x_{k-1}$ by : (Ref. (30))

$$f(x) = G_k \frac{(x - x_{k-1})^3}{6\,\ell_k} + G_{k-1} \frac{(x_k - x)^3}{6\,\ell_k} + \left(\frac{r_k}{\ell_k} - G_k \frac{\ell_k}{6}\right)(x - x_{k-1}) + \left(\frac{r_{k-1}}{\ell_k} - G_{k-1} \frac{\ell_k}{6}\right)(x_k - x) \qquad (4.3)$$

where $k = 1,2,3,\ldots,N$.

The gradient at any point in the just fitted spline is computed from

$$f'(x) = G_k \frac{(x - x_{k-1})^2}{2\,\ell_k} - G_{k-1} \frac{(x_k - x)^2}{2\,\ell_k} + \left(\frac{r_k}{\ell_k} - G_k \frac{\ell_k}{6}\right) - \left(\frac{r_{k-1}}{\ell_k} - G_{k-1} \frac{\ell_k}{6}\right) \qquad (4.4)$$

The next step is to replace the ordinates $r_1, r_2, \ldots, r_k$ by the slopes $f'(x_1)$, $f'(x_2)$, $f'(x_3)$ ... $f'(x_N)$ respectively. A second spline is then made to pass through the new set of points $(x_1, f'(x_1))$, $(x_2, f'(x_2)), \ldots, (x_N, f'(x_N))$. This second spline can be defined in the interval ℓ_k by :

$$F(x) = Q_k \frac{(x - x_{k-1})^3}{6\,\ell_k} + Q_{k-1} \frac{(x_k - x)^3}{6\,\ell_k} + \left(\frac{f'(x_k)}{\ell_k} - Q_k \frac{\ell_k}{6}\right)(x - x_{k-1}) + \left(\frac{f'(x_{k-1})}{\ell_k} - G_{k-1} \frac{\ell_k}{6}\right)(x_k - x) \qquad (4.5)$$

Again, the gradient at any point in this spline is given by :

$$F'(x) = Q_k \frac{(x - x_{k-1})^2}{2\,\ell_k} - Q_{k-1} \frac{(x_k - x)^2}{2\,\ell_k} + \left(\frac{f'(x_k)}{\ell_k} - Q_k \frac{\ell_k}{6}\right) - \left(\frac{f'(x_{k-1})}{\ell_k} - Q_{k-1} \frac{\ell_k}{6}\right) \qquad (4.6)$$

The curvature at a typical point (x_k, r_k) is thus

$$\left(\frac{1}{r_m}\right)_k = F'(x_k) / \left[1 + \{f'(x_k)\}^2\right]^{3/2} \qquad (4.7)$$

The coefficients G and Q are evaluated by matching the slopes and curvatures, of the spline, of adjoining intervals at their common points. This leads to the solution of a diagonal matrix, which is easily done on a computer. Two end constants have to specified and the choice made here is that used by Katsanis (4). The second derivative at either end point is chosen one-half that at the adjacent point. This provides the two equations necessary to complete the set of equations for the solution.

4.4 Over-all Program logic

The computer program is composed of a main routine and twenty two subroutines. A list of these subroutines along with their main functions is given below.

1. INPUT - to print all the input data.
2. STRAC - to calculate the slopes and curvatures of the hub and casing streamlines .

3. SPECHT – to determine the specific heat at constant pressure, specific heat ratio, and related parameters at each station.

4. POWER – to determine the drop in absolute total temperature across each streamline of a rotor when the work done by the turbine is specified.

5. POWER 1 – to determine the drop in absolute total temperature across each streamline of a rotor when the rotor relative exit angles are specified.

6. SPRIP – to obtain the initial estimate of the radial position of each streamline.

7. STRVAL – to obtain streamline values of the items required for the solution of the radial equilibrium equation.

8. VMRTL – to obtain an initial estimate of the meridional velocity at the mean streamline.

9. RADVEL – to control the logic of the calculation of the meridional velocity distribution.

10. RUNKUT – contains the algorithm for the Runge-Kutta-Gill method of solving a first-order ordinary differential equation.

11. DERIV – to obtain a value of the derivative of the square of the meridional velocity with respect to the radial position for a specified

- velocity and radial position.

12. V.SUB - to obtain a new estimate of the meridional velocity at the mean streamline.

13. REMAIN - to obtain streamline values for the quantities tabulated in the output which have not already been obtained.

14. SETUP - to obtain streamline values of quantities for calculations at the next station. It also calculates the mass averaged values which are to be printed in the output.

15. OUTPUT - to print the results of the calculation.

16. PLC - evaluates the total-pressure-loss-coefficient for each streamline using the loss model of Carter, et. al. (16).

17. PLC1 - evaluates the total-pressure-loss coefficient for each streamline using the loss model developed in this work.

18. LCNV - estimates the total-pressure-loss coefficient from the kinetic-energy-loss coefficient when they are specified.

19. SPLINE - evaluates streamline slopes and curvatures by fitting spline curves through the estimated streamline radial positions.

20. I1AP1 - is to perform parabolic interpolation of a tabulated function of one variable. If

parabolic interpolation is not possible, linear interpolation or extrapolation of a single value is performed.

21. SLOPE - to obtain the derivative of a tabulated function with respect to an independent variable at each tabular entry.

22. SLEQ - solution of a set of simultaneous linear algebraic equations by the Gauss method, with pivoting.

An over-all flow diagram for the program is given in Figure 4. It can be seen that the over-all control of the calculation procedure is maintained by the main routine while subroutine RADEQL maintains control over the calculation procedure for the meridional velocity distribution.

CHAPTER 5

APPLICATIONS AND DISCUSSION

The computer program was used to the predict the performance of several single and multistage turbines. The results of these applications are presented in this chapter.

To debug the computer program the results presented by Carter, et. al.(29) were duplicated. This cleared any possible errors in the basic computer program. Necessary modifications were then made to the program in steps and the modifications debugged at each stage.

To study the effects of the radial disturbution of losses on the solution, efficiencies were prescribed in the initial program runs. This provided a useful insight into the effects of the loss distribution on the solution. The first of the problems encountered was in the prescription of the work distribution along the blade height. The turbines under consideration were designed with a constant loss all along the blade height. Consequently when a radial distribution of the loss was prescribed, the design work distribution was no longer valid. This was immediately evident in initial program runs by an inability to find a valid solution to the radial equilibrium equation in the hub and tip regions due to overloading of these sections. Since the efficiencies prescribed in the

hub and tip regions were lower than the average efficiency used in the design of the turbine, to obtain the design work larger turning of the flow at these sections was required and consequent overloading. To overcome this problem required a redistribution of the work done along the blade height till the rotor exit flow angles closely matched the design angles. This proved a cumbersome procedure. The use of the rotor exit flow angle instead of the work distribution as an input to the program was an obvious solution and a subroutine was added to facilitate this option.

The use of radial loss distributions introduced large gradients in the flow properties which increased as the calculation proceeded downstream till their profiles were so distarted that a solution was no longer possible. However, such a situation would not occur in real flows. Mixing of the flow would tend to straighten out this gradient. The simple mixing model described in Chapter 4 was used to simulate the effects of mixing. It was found that prescribing 50% mixing in the flow for each stage produced the best results. This level of mixing was maintained in all program runs, the results of which are presented here.

4.1 Test case 1

A single stage turbine with large hub-to-tip radius ratio was used as the first test case (Ref [illegible] Design

details of this turbine are presented in Figure 5. The program was run with a prescribed work distribution, prescribed rotor relative exit angles for the present loss model and the loss model of Ref. (16).

Figures (6) and (7) present the radial distribution of outlet flow angle and stagnation pressure distribution. Both these distributions are predicted well by both the loss models. This indicates that the effect of the loss distribution is less important in the case of large hub-to-tip radius ratio turbines, i.e., turbines with small blade heights. Figure (8) compares the efficiency distribution of the two loss models. The figure clearly shows the difference between their loss distributions. The present loss model shows a maximum efficiency around the mean line as would be expected in an axial turbine while the loss model of Ref. (16) shows a maximum efficiency at the blade tip which is unlikely to occur in such turbines.

Table 1 compares the predicted overall performance parameters with experimentally measured values. The loss model of Ref. (16) predicts a higher efficiency and lower pressure ratio while the present loss model predicts a lower efficiency and more accurate pressure ratio. Better prediction of the wall static pressure is also indicated by the present loss model.

	Experimental	Present loss model (work specification	Present loss model (angle specification)	Loss model of Ref.(16) (work specification)
Turbine total efficiency	0.92	0.89	0.89	0.93
Total-to-Total Pressure ratio	1.909	1.897	1.909	1.847
Hub static pressure	0.455	0.462	0.463	0.481
Tip static pressure	0.445	0.461	0.462	0.480

4.2 Test Case 2

A two stage turbine designed for a low cost turbofan engine was used for this test case (Ref. 32). Design details of the turbine are presented in Figure (9). The program was run using a specified work distribution with the present loss model and specified relative exit angles for the loss model of Ref.(16)

The radial distribution of the outlet flow angles at first and second stage exits predicted by the two loss models are compared with experimentally measured values (Figures (10) and (11) respectively). It is evident that the present loss model shows an improved prediction of the trend of the first stage outlet flow angle. Large deviations of the predicted outlet flow angle at the second stage exit, in the hub and tip regions, from the experimentally measured values are seen in Figure (11). However, Ref. (32) points out that the measurements showed a large amount

of underturning in these regions. A large amount of turning at these sections would have resulted in a distribution close to that predicted by the present loss model.

Table 2 compares overall performance parameters predicted by the two loss models with experimentally measured values. The loss model of Ref. (16) predicts a very low total pressure ratio.

Table 2

	Experimental	Loss of model of Ref. (16)	Present loss model
Turbine total efficiency	0.93	0.9073	0.914
Turbine static efficiency	0.80		0.777
Total-to-total pressure ratio	3.75	2.525	3.51
Total-to-static pressure ratio	4.6	2.845	4.63
Stage one total efficiency	0.93	0.95	0.908
Stage two total efficiency	0.91	0.83	0.903

4.3 Test Case 3

A three stage turbine with very high stage loading was used for the third test case. Design details of this turbine are presented in Ref. (33) and the results of

experimental investigation in Ref. (34). Some of the design details are presented in Figure(12). The program was run with specified rotor relative exit angles.

The predicted radial distributions of the Total-to-Total efficiency for the first, second, and third stage exits are compared with experimental results in Figures (13), (14) and (15) respectively. Good agreement is shown in all the cases. The deviation of the efficiency level at the mean line suggests that the estimated profile loss using the Ainley-Mathieson correlation is too high (Horlock (20)). The predicted wall static pressure distributions compare very well with the experimental results (Figure (16)). The predicted outlet flow angle distribution (Figure (17)) shows deviations from the experimentally measured values in the hub and tip regions. Deviations of the same order are also seen in the results presented by Hirsch (7) and larger deviations in the results of Renaudin and Somm (14), for other turbines.

Attempts at obtaining a solution using the loss model of Ref. (16) failed in this test case. The apparent reason was that with highly loaded turbines, the solution is sensitive to the radial distribution of losses.

Table 3 compares the predicted overall performance parameters with experimental results. Good agreement is seen with the experimental results.

Table 3

	Experimental value	Predicted
Turbine total efficiency	0.886	0.867
Turbine work output	3018.93 HP	2952.81 HP
Total pressure ratio	3.48	3.42
Total-to-static pressure ratio	3.843	3.839

4.4 Test Case 4

A four stage turbine with very high stage loading was used for the fourth test case. Design details of this turbine are presented in Ref. (35) and the results of experimental investigations on it in Ref. (36). Some of the design details are presented here in Figure (18). The program was run with the rotor relative exit angles specified.

Figure (19) compares the radial distribution of the Total-to-Total efficiency with the experimental measurements. While the trend of the experimentally measured distribution has been predicted well, the overall efficiency level predicted is lower by about 2% . Once again, the difference in efficiencies at the mean line would indicate a too high profile loss predicted by the present loss model. Good prediction in the trends of the radial distribution of the stagnation pressure and outlet flow angle are seen from Figures (20) and (21) respectively. The lower stagnation

pressure could be due to the lower predicted efficiencies. The deviations in the outlet flow angle are of the same order as the results shown by Hirsch (7) for other turbines. Good prediction of the wall static pressure distribution is seen from Figure (22).

Table 4 compares the predicted overall performance parameters with experimental results. As mentioned earlier, the predicted overall efficiency is lower than the measured value.

Table 4

	Experimental	Predicted
Turbine total efficiency	0.853	0.835
Turbine work output	3400.00 HP	3380.10 HP
Total-to-Total pressure ratio	2.66	2.875
Total-to-static pressure ratio	2.955	3.221

Results obtained from initial program runs using a prescribed efficiency distribution are presented in Figures (23) and (24). Good agreement with experimental results in all cases showed the importance of the loss distribution on the predictions. In a bid to study the effect of a change in the prescribed mixing pattern, Figure (25) shows the effect on the static pressure distribution of prescribing the mixing

coefficients by two methods. Very little difference is observed by prescribing 50% mixing at stage exits and prescribing 30% mixing at all blade row exists.

Attempts at obtaining solutions using the loss model of Ref. (16) failed in this test case also.

To substantiate the statement that the deviation in the results is due to the high profile loss from the Ainley-Mathieson correlation, the program was run after reducing the profile losses computed with the above correlation by 20% . Secondary losses were kept unchanged Figures (26) and (27) show the new radial distributions of total pressure and outlet flow angle compared with experimental measurements. Considerable improvement in the predictions are seen as a result of the above modification in the loss correlation.

CHAPTER 6

CONCLUSIONS

1. An attempt has been in the present investigations to evaluate different loss models for axial turbines in a streamline curvature computing scheme using the full radial equilibrium equation. Four single and multistage turbines have been analysed. The design details and measured data were available for these turbines.
2. The loss model proposed in this work to take into account the radial distribution of losses in the annulus has been very successful. The predicted wall static pressure distributions and the radial distributions of stagnation pressure and efficiency agree very well with the measured ones.
3. The loss model of Carter,et. al (16) failed to produce solutions for highly loaded multistage turbines. This may be attributed to a radial distribution of losses quite different from those obtained in practice. This model also predicts an overall efficiency which is higher than the measured one.
4. It was observed that the Ainley-Mathieson correlation predicted too high a value of profile loss for modern turbines. This lead to a prediction of a lower overall efficiency for the test turbines. A reduction in the level of the profile loss produced considerable improvements in the results.

5. The evaluation of the streamline slopes and curvatures from the hub and casing slopes and curvatures was found satisfactory in view of the good predictions obtained for multistage turbines.

6. Several modifications have been made to the computer program of Carter, et. al (29). The addition of rotor relative exit angle subroutine has made it suitable for both analysis and design computations.

Appendix A

An expression for the term $D\,V_m/Dm$ in the radial equilibrium equation

The continuity equation can be written as :

$$\frac{\vec{W}}{\rho}\frac{D\rho}{Ds} + \nabla \cdot \vec{W} = 0 \qquad (A1)$$

In cylindrical co-ordinates,

$$\nabla \cdot \vec{W} = \frac{1}{r} \cdot \frac{\partial (r W_r)}{\partial r} + \frac{\partial W_u}{r\partial\theta} + \frac{\partial W_x}{\partial x} \qquad (A2)$$

Also, the derivative of a quantity in the direction of flow (the s-direction) at any instant in time may be expressed by :

$$\frac{\partial(\ )}{\partial s} = \frac{W_r}{W} \cdot \frac{\partial(\ )}{\partial r} + \frac{W_u}{W} \frac{\partial(\ )}{r\partial\theta} + \frac{W_x}{W} \cdot \frac{\partial(\ )}{\partial x} \qquad (A3)$$

or re-arranging,

$$\frac{\partial(\ )}{\partial x} = \frac{W}{W_x} \cdot \frac{\partial(\ )}{\partial s} - \frac{W_r}{W_x} \cdot \frac{\partial(\ )}{\partial r} - \frac{W_u}{W_x} \cdot \frac{\partial(\ )}{r\partial\theta} \qquad (A4)$$

Use equation (A4) in (A2) to eliminate the x derivative.

We get

$$\nabla \cdot \vec{W} = W_x \left[\frac{1}{r} \cdot \frac{\partial}{\partial r} \left(\frac{rW_r}{W_x}\right) + \frac{\partial}{r\partial\theta} \left(\frac{W_u}{W_x}\right) \right] + \frac{W}{W_x} \cdot \frac{\partial W_x}{\partial x} \qquad (A5)$$

Since,

$$\frac{W_r}{W_x} = \tan\phi \quad \text{and} \quad \frac{W_u}{W_x} = \tan\beta$$

equation (a5) can be rewritten as

$$\nabla \cdot \vec{V} = W_x \left[\frac{1}{r} \cdot \frac{\partial (r \tan \phi)}{\partial r} + \frac{\partial \tan \beta}{r \partial \theta} \right] + \frac{V}{W_x} \cdot \frac{\partial W_x}{\partial x} \qquad (A6)$$

It is known that

$$\frac{D(\ )}{Dt} = \frac{\partial (\ )}{\partial t} + V \frac{\partial (\ )}{\partial s} \qquad (A7)$$

Along with the kinematic relation $\frac{D(\ )}{Dt} = V \frac{D(\ )}{Ds}$, equation (A7) can be written

$$\frac{\partial (\ )}{\partial x} = \frac{D(\ )}{Ds} - \frac{1}{V} \cdot \frac{\partial (\ )}{\partial t} \qquad (A8)$$

Equation (A8) can be used for the last term of equation (A6). Also since

$$V_x = W_m \cos \phi \qquad (A9)$$

we get,

$$\frac{\partial V_x}{\partial s} = \frac{D}{Ds} (W_m \cos \phi) - \frac{1}{V} \cdot \frac{\partial W_x}{\partial t} \qquad (A10)$$

We also know that

$$W \frac{D(\ )}{Ds} = W_m \frac{D(\ )}{Dm} \qquad (A11)$$

Thus,

$$\frac{\partial W_x}{\partial s} = \frac{W_m^2}{V} \cdot \frac{D \cos \phi}{Dm} + \cos \phi \frac{W_m}{V} \cdot \frac{DW_m}{Dm} - \frac{1}{V} \cdot \frac{\partial W_x}{\partial t} \qquad (A12)$$

Substitute equation (A12) in (A6), we get

$$\nabla \cdot \vec{V} = W_x \left[\frac{1}{r} \cdot \frac{\partial (r \tan \phi)}{\partial r} + \frac{\partial \tan \beta}{r \partial \theta} \right] + W_r \frac{\sec \phi}{r_m} + \frac{DW_m}{Dm} - \frac{1}{W_x} \cdot \frac{\partial W_x}{\partial t} \qquad (A13)$$

For an axisymmetric, steady flow

$$\nabla \cdot \vec{W} = W_x \frac{1}{r} \frac{\partial(r \tan \phi)}{\partial r} + W_r \frac{\sec \phi}{r_m} + \frac{DW_m}{Dm} \qquad (A14)$$

We next apply the momentum equation in the flow direction

$$-\frac{1}{\rho} \cdot \frac{\partial p}{\partial s} = \frac{D}{Dt}\left(\frac{W^2}{2}\right) - \omega^2 rW \qquad (A15)$$

Using equations (A8) and (A11), (A15) can be written as

$$-\frac{W}{\rho} \cdot \frac{Dp}{Ds} + \frac{1}{\rho} \cdot \frac{\partial p}{\partial t} = W_m^2 \frac{DW_m}{Dm} + W_u W \frac{DW_u}{Dx} - \omega^2 rW \qquad (A16)$$

This can be rewritten as

$$-\frac{1}{\rho} \cdot \frac{Dp}{Ds} = W_m^2 \frac{DW_m}{Dm} - W_r \frac{V_u^2}{r} - \frac{W_u}{\rho} \cdot \frac{\partial p}{r\partial\theta} - \frac{1}{\rho} \cdot \frac{\partial p}{\partial t} \qquad (A17)$$

For an axisymmetric, steady flow

$$-\frac{1}{\rho} \cdot \frac{Dp}{Ds} = W_m^2 \frac{DW_m}{Dm} - W_r \frac{V_u^2}{r} \qquad (A18)$$

Also,

$$\frac{Dp/Dp}{Dp/Ds} = a^2 \qquad (A19)$$

This relation along with equation (A1), (A14), and (A18) can be used to obtain an expression for Dw_m/Dm that does not contain $\nabla \cdot \vec{W}$, Dp/Ds or Dp/Ds. We get

$$\frac{1}{a^2}\left[W_r \frac{V_u^2}{r} - W_m^2 \frac{DW_m}{Dm}\right] + \frac{W_x}{r} \cdot \frac{\partial(r \tan \phi)}{\partial r} + W_r \frac{\sec \phi}{r_m} + \frac{DW_m}{Dm} = 0 \qquad (A20)$$

Using the definition of Mach number, $M_m = W_m/a$ and $M_\theta = V_u/a$ in equation (A20) and rearranging, we get

$$(1 - M_m^2)\ \frac{DV_m}{Dm} = W_m \left[\frac{M_\theta^2}{r} \sin\phi + \frac{\tan\phi}{r_m} + \frac{\sin\phi}{r} + \frac{1}{\cos\phi} \cdot \frac{\partial\phi}{\partial r}\right] \tag{A21}$$

Since $W_m = V_m$, equation (A21) can be rewritten as

$$\sin\phi\ \frac{DV_m}{Dm} = \frac{V_m \left[\left(1 + M_\theta^2 + \frac{r}{r_m \cos\phi}\right) \frac{\sin^2\phi}{r} + \tan\phi\ \frac{\partial\phi}{\partial r}\right]}{(1 - M_m^2)} \tag{A22}$$

Appendix B

Evaluation of the total temperature drop across a stage

When the total power output of a stage is specified, the total temperature distribution at a stage exit will have to satisfy both the specified power output and its distribution across the annulus. Since initially the distribution of mass flow throughout the annulus is unknown until the distribution of meridional velocity has been established, the power distribution is specified by nondimensional power functions versus the nondimensional mass flow function, w(r), defined below

$$w(r) = \frac{2\pi \int_{r_h}^{r} \rho V_x \, r \, dr}{w_T} \qquad (A23)$$

If the total power output specified is HP_T (horsepower), the total temperature drop ΔT_o through the rotor must satisfy the equation,

$$HP_T = 5.6925 \, c_p \int_o^{w_T} \Delta T_o \, dw \qquad (A24)$$

Normalizing equation (A24) with respect to the total power and the total mass flow, leads to a definition of the power function P(w(r)) expressed as

$$P(w(r)) = 5.6925 \, w_T \, c_p / HP_T \int_o^{w(r)} \Delta T_o \, d\, w(r) \qquad (A25)$$

Differentiating equation (A25) with respect to the non-dimensional mass flow function yields an expression for the total temperature drop, for the jth streamline,

$$(\Delta T_o)_j = \frac{HP_T}{5.6935\, w_T\, c_{p_j}} \left[\frac{dP(w(r))}{dw(r)} \right] \qquad (A26)$$

The power function versus the mass flow function will be a basic specification for power distribution from which the total temperature drops are obtained.

When the rotor relative exit angles are specified, the total temperature drops are obtained from the Euler work equation

$$(\Delta T_o)_j = \left[\frac{V_{u1}\, u_1 - V_{u2}\, u_2}{c_p} \right]_j \qquad (A27)$$

Appendix C

Coefficients of the differential equations

To simplify the logic of the computer program, a standard procedure has been adopted for the solution of the flow field at each inter blade row station. The different types of stations and the various optional specifications are taken into account by modifications to the twelve coefficients appearing in the three differential equations (Equations 2.30, 2.31, and 2.32). This appendix presents these coefficients.

First station inlet

$$C_{11} = 1.0$$

$$C_{12} = \left(\frac{\gamma-1}{\gamma}\right)\left[V_{uo}^2 + V_{mo}^2 - 2c_p T_{oo}\right]$$

$$C_{13} = 2V_{uo}$$

$$C_{14} = \frac{2V_{mo}^2}{V_m}\cos\phi_o - \frac{2V_{uo}^2}{r} + \left(V_{uo}^2 + V_{mo}^2\right)\frac{1}{T_{oo}}\cdot\frac{dT_{oo}}{dr} + V_{mo}\sin\phi_o\frac{\partial V_{mo}}{\partial m}$$

The total pressure would be a specified function of radius. Hence, the coefficients of equation (2.31) are

$$C_{21} = 0$$

$$C_{22} = 1.0$$

$$C_{23} = 0$$

$$C_{24} = \frac{1}{p_{oo}} \cdot \frac{dp_{oo}}{dr}$$

$$C_{31} = -\frac{\tan \beta_o \cos \phi_o}{2V_{mo}}$$

$$C_{32} = 0$$

$$C_{33} = 1.0$$

$$C_{34} = V_{mo} \left[\frac{\cos \phi_o}{\cos^2 \beta_o} \frac{d\beta_o}{dr} - \tan \beta_o \sin \phi_o \frac{d\phi_o}{dr} \right]$$

Stator exit

$$C_{11} = 1.0$$

$$C_{12} = \left(\frac{\gamma-1}{\gamma}\right) \left[V_{u1}^2 + V_{m1}^2 - 2c_p T_{o1} \right]$$

$$C_{13} = 2V_{u1}$$

$$C_{14} = \frac{2V_{m1}^2 \cos \phi_1}{r_m} - \frac{2V_{u1}^2}{r} + (V_{u1}^2 + V_{m1}^2) \frac{1}{T_{o1}} \frac{dT_{o1}}{dr} + V_{m1} \sin \phi_1 \frac{DV_{m1}}{Dm}$$

Assuming that the derivative $\frac{dY_N}{dr}$ can be expressed as

$$\frac{dY_N}{dr} = C_{Y1} \frac{dV_{m1}^2}{dr} + C_{Y3} \frac{dV_{u1}}{dr} + C_{Y4}$$

the coefficients of equation (2.31) become

$$C_{21} = \frac{\left(\frac{p_{o1}}{p_{oo}}\right) \left(\frac{T_1}{T_{o1}}\right)^{\frac{1}{\gamma-1}}}{2R\, T_{o1}} Y_N + \left(\frac{p_{o1}}{p_{oo}}\right)\left(1 - \frac{p_1}{p_{o1}}\right) C_{Y1}$$

$$C_{22} = 1.0$$

$$C_{23} = \frac{V_{u1} \left(\frac{p_{o1}}{p_{oo}}\right) \left(\frac{T_1}{T_{o1}}\right)^{\frac{1}{\gamma-1}}}{R\, T_{o1}} + \left(\frac{p_{o1}}{p_{oo}}\right) \left(1 - \frac{p_1}{p_{o1}}\right) C_{Y3}$$

$$C_{24} = \frac{1}{p_{oo}} - \frac{d\rho_{oo}}{dr} + \frac{\left(\frac{p_{o1}}{p_{oo}}\right) \left(\frac{T_1}{T_{o1}}\right)^{\frac{1}{\gamma-1}}}{2R\, T_{o1}} \left(V_{u1}^2 + V_{m1}^2\right) \frac{\gamma_N}{T_{o1}} \frac{dT_{o1}}{dr}$$

$$- \left(\frac{p_{o1}}{p_{oo}}\right) \left(1 - \frac{p_1}{p_{o1}}\right) C_{Y4}$$

$$C_{31} = - \frac{\tan \beta_1 \cos \phi_1}{2V_{m1}}$$

$$C_{32} = 0$$

$$C_{33} = 1.0$$

$$C_{34} = V_{m1} \left[\frac{\cos \phi_1}{\cos^2 \beta_1} \frac{d\beta_1}{dr} - \tan \beta_1 \sin \phi_1 \frac{d\phi_1}{dr} \right]$$

Stage exit

$$C_{11} = 1.0$$

$$C_{12} = \left(\frac{\gamma}{\gamma-1}\right) \left[V_{u2}^2 + V_{u2}^2 - 2c_p T_{o2} \right]$$

$$C_{13} = 2V_{u2}$$

$$C_{14} = \frac{2V_{m2}^2 \cos \phi_2}{r_m} - \frac{2V_{u2}^2}{r} + \left(V_{u2}^2 + V_{m2}^2\right) \frac{1}{T_{o2}} \cdot \frac{dT_{o2}}{dr}$$

$$+ V_{m2} \sin \phi_2 \frac{DV_{m2}}{Dm} .$$

Again, assuming that the derivative $\frac{dY_R}{dr}$ can be expressed as

$$\frac{dY_R}{dr} = C_{Y1} \frac{dV_{m2}^2}{dr} + C_{Y3} \frac{dV_{u2}}{dr} + C_{Y4}$$

the coefficients of equation (2.31) are

$$C_{21} = \frac{(\frac{p'_{o2}}{p'_{o2s}})Y_R}{2R\ T_2} + (\frac{p'_{o2}}{p'_{o2s}})\ (1 - \frac{p_2}{p'_{o2}})\ C_{Y1}$$

$$C_{22} = 1.0$$

$$C_{23} = \frac{V_{u2}(\frac{p'_{o2}}{p'_{o2s}})Y_R}{R\ T_2} - \frac{u_2\left[1 - (\frac{p'_{o2}}{p'_{o2s}})Y_R\right]}{R\ T'_{o2}} + (\frac{p'_{o2}}{p'_{o2s}})\ (1 - \frac{p_2}{p'_{o2}})\ C_{Y3}$$

$$C_{24} = \frac{1}{p'_{o1}} \frac{dp'_{o1}}{dr} + \frac{1}{2R\ T'_{o2}}\left[2u_2\ \omega - wu_1\ \omega - (u_2^2 - u_1^2)\ \frac{1}{T'_{o1}} \frac{dT'_{o1}}{dr}\right]$$

$$- \frac{(1 + \frac{p'_{o2}}{p'_{o2s}}\ Y_R)}{2R\ T'_{o2}}\left[2u_2\ \omega - 2V_{u2}\ \omega - (u_2^2 - 2u_2\ V_{u2})\ \frac{1}{T_{o2}} \frac{dT_{o2}}{dr}\right]$$

$$+ \frac{Y_R\ (\frac{p'_{o2}}{p'_{o2s}})}{2R\ T_2} (V_{m2}^2 + V_{u2}^2)\ \frac{1}{T_{o2}} \frac{dT_{o2}}{dr}$$

$$- (\frac{p'_{o2}}{p'_{o2s}})\ (1 - \frac{p_2}{p'_{o2}})\ C_{Y4}.$$

When the work output of the turbine is specified, V_{u2} is in effect a known function of radius. Thus,

$$C_{31} = 0$$

$$C_{32} = 0$$

$$C_{33} = 1.0$$

$$C_{34} = \frac{dV_{u2}}{dr}$$

When the rotor relative exit angles are specified, the coefficients of equation (2.32) are similar to those at the stator exit.

$$C_{31} = -\frac{\tan \beta'_2 \cos \phi_2}{2 V_{m2}}$$

$$C_{32} = 0$$

$$C_{35} = 1.0$$

$$C_{34} = V_{m2} \left[\frac{\cos \phi_2}{\cos^2 \beta'_2} \frac{d\beta'_2}{dr} - \tan \beta'_2 \sin \phi_2 \frac{d\phi_2}{dr} \right] + u_2$$

Appendix D

The Runge-Kutta-Gill method for the solution of ordinary differential equations

The differential equation is of the form

$$dV_m^2/dr = f(r, V_m)$$

where $f(r,V_m)$ is obtained from the simultaneous solution of the radial equilibrium equation and two subsidiary differential equations.

Given the value of the meridional velocity at one streamline, $(V_{mi})_j$, the unknown value at the adjacent streamline, $(V_{mi})_k$, is determined in four stages :

$$(1) \qquad (V_{mi})^2_{k1} = (V_{mi})^2_j + \frac{1}{2}(k_1 - 2q_o)$$

where $k_1 = hf\{r_{ij}, (V_{mi})_j\}$

$$q_o = \begin{cases} 0 & \text{initially} \\ q_4 & \text{subsequently} \end{cases}$$

$h = r_{i,k} - r_{ij}$

$$(2) \qquad (V_{mi})^2_{k2} = (V_{mi})^2_{k1} + \left(1 - \frac{1}{\sqrt{2}}\right)(k_2 - q_1)$$

where $k_2 = hf\{r_{ij} + h/2, (V_{mi})_{k1}\}$

$$q_1 = q_o + 3\left[\frac{1}{2}(k_1 - 2q_o)\right] - \frac{1}{2}k_1$$

(3) $$(V_{mi})^2_{k3} = (V_{mi})^2_{k2} + \left(1 + \frac{1}{\sqrt{2}}\right)(k_3 - q_2)$$

where $k_3 = hf\{r_{ij} + h/2,\ (V_{mi})_{k2}\}$

$$q_2 = q_1 + 3\left[\left(1 - \frac{1}{\sqrt{2}}\right)(k_2 - q_1)\right] - \left(1 - \frac{1}{\sqrt{2}}\right) k_2$$

(4) $$(V_{mi})^2_{k} = (V_{mi})^2_{k3} + \frac{1}{6}(k_4 - 2q_2)$$

where $k_4 = hf\{r_{ik},\ (V_{mi})_{k3}\}$

$$q_3 = q_2 + 3\left[\left(1 + \frac{1}{\sqrt{2}}\right)(k_3 - q_2)\right] - \left(1 + \frac{1}{\sqrt{2}}\right) k_3$$

$$q_4 = q_3 + 3\left[\frac{1}{6}(k_4 - 2q_3)\right] - \frac{1}{2} k_4 .$$

References

1. Wu, C.-H., 'A general theory of three-dimensional flow in subsonic and supersonic turbomachines of axial-, radial-, and mixed-flow type', NACA TN 2604 (1952).

2. Marsh, H., 'A digital computer program for the through flow fluid mechanics in an arbitrary turbomachine using a matrix method', Aeronautical Research Council, R and M 3509 (1966).

3. Biniaris, S., 'The calculation of the Quasi-Three Dimensional flow in an axial gas turbine', J. of Engg. for Power, April 1975.

4. Katsanis, T., and McNally, W.D., 'Fortran program for calculating velocities and streamlines on the hub-shroud mid-channel flow surface of an axial- or mixed-flow turbomachine, I-User's manual', NASA TN D-7343 (1973).

5. Bosman, C., and Marsh, H., 'An improved method for the calculation of the flow in turbomachines, including a consistent loss model' J. of Mech. Engg. Sci., Vol. 16, Feb. 1974.

6. Hirsch, Ch., and Warzee, G., 'A finite element method for the axisymmetric flow computation in a turbomachine', Int. J. for Numerical Methods in Engg., Vol. 10, 1976.

7. Hirsch, Ch., 'Finite element method for through-flow calculations', Conference proceedings No. 195 on through-flow calculations in axial turbomachinery', AGARD.

8. Smith, L.H., Jr., 'The radial-equilibrium equation of turbomachinery' J. of Engg. for Power, Jan. 1966.

9. Novak, R.A., 'Streamline curvature computing procedures for fluid flow problems', J. of Engg. for Power, Oct.1967.

10. Jansen, W., and Moffat, J.C., 'Off design analysis of axial flow compressors', J. of Engg. for Power, Oct. 1967.

11. Lieblein, S., 'Loss and stall analysis of compressor cascades', J. of Basic Engg., Vol. 81, Series D, 1959.

12. Frost, D.H., 'A streamline curvature through-flow computer program for analysing the flow through axial flow turbomachines', Aeronautical Research Council, R and M 3687, Aug. 1970.

13. Novak, R.A., and Hearsey, R.M., 'A nearly three-dimensional computing system for turbomachinery, Part I and II', ASME Paper No. 76-FE-20, March 1976.

14. Renaudin, A., and Somma, E., 'Quasi-three-dimensional flow in a multistage turbine calculation and experimental verification', Flow Research on Blading, Ed. Dzung, L.S., Elsevier Publishing Company.

15. Silvester, M.E., and Hetherington, R., 'A numerical solution of the three-dimensional compressible flow through axial turbomachinery', Numerical Analysis - An Introduction, Edited by J. Welsh, Academic Press (1966).

16. Carter, A.F., Platt, M., and Lenherr, F.K., 'Analysis of geometry and design point performance of axial flow turbines, Part I - Development of the analysis method and the loss coefficient correlation', NASA CR 1181, Sept. 1968.

17. Smith, S.F., 'A simple correlation of turbine efficiency', J. Royal Aero. Soc., Vol. 69, July 1965.

18. Davis, W.R., and Millar, D.A.J., 'A comparison of the Matrix and Streamline curvature methods of axial flow turbomachinery analysis, From a user's point of view', J. of Engg. for Power, Oct. 1975.

19. Majumdar, A.S., 'A review of recent computational procedures for off-design analysis of axial compressors', J. of the Aero. Soc. of India, Vol. 27,No.1, Feb. 1975.

20. Horlock, J.H., 'Axial flow turbines', Butterworths Pub., 1966.

21. Jansen, W., 'A method for calculating the flow in a centrifugal impeller when entropy gradients are present', Internal Aerodynamics (Turbomachinery), Pub. Institution of Mechanical Engineers, London.

22. Horlock, J.H., 'On entropy production in adiabatic flow in turbomachines', J. of Basic Engg., 1971.

23. Wu, C.H., 'Three-dimensional turbomachine flow equations expressed with respect to non-orthogonal curvilinear coordinates and methods of solution', Proceedings - 3rd International Symposium on Air Breathing Engines, March 1976.

24. Hanley, T.T., 'A correlation of end wall losses in plane compressor cascades', J. of Engg. for Power, July 1968.

25. Balje, O.E., and Binsley, R.L., 'Axial turbine performance evaluation, Part A - loss geometry relationships', J. of Engg. for Power, Oct. 1968.

26. Tabakoff, W., and Hosny, W., 'An experimental investigation on loss reduction in small guide vanes', AIAA Paper no. 76-617, 1976.

27. Dunham, J., 'A review of cascade data on secondary losses in turbines', J. of Mech. Engg. Sci., Vol. 12, No. 1, 1970.

28. Dunham, J., and Came, P.M., 'Improvements to the Ainley-Mathieson method of turbine performance prediction', J. of Engg. for Power, July 1970.

29. Carter, A.F., and Platt, H., 'Analysis of geometry and design point performance of axial flow turbines, Part II - computer program', NASA CR-1187, Oct. 1968.

30. Daneshywar, 'A critical assessment of methods of calculating slope and curvature of streamlines in fluid flow problems', Proc. Inst. of Mech. Eng., Vol. 186, 70/72.

31. Kofskey, M.G., Roelke, J.R., and Haas, E.J., 'Turbine for a low cost turbojet engine, Part II - opened stator', NASA TN D-7625.

32. Kofskey, M.G., and Nusbaum, W.J., 'Design and cold-air investigation of a turbine for a small low-cost turbofan engine', NASA TN D-6967.

33. Evans, D.C., and Wolfmeyer, G.W., 'Highly loaded multistage fan drive turbine - plain blade design configuration', NASA CR 196-, 1972.

34. Wolfmeyer, G.W., and Thomas, M.W., 'Highly loaded multistage fan drive turbine - performance of initial seven configurations', NASA CR 2362, 1974.

35. Evans, D.C., and Hill, J.M., 'Experimental investigation of a $4\frac{1}{2}$-stage turbine with very high stage loading factor, I - turbine design', NASA CR-2140, 1973.

36. Walker, M.D., and Thomas, M.W., 'Experimental investigation of a $4\frac{1}{2}$ - stage turbine with very high loading factor, II-^{2} turbine performance', NASA CR-2363, 1974.

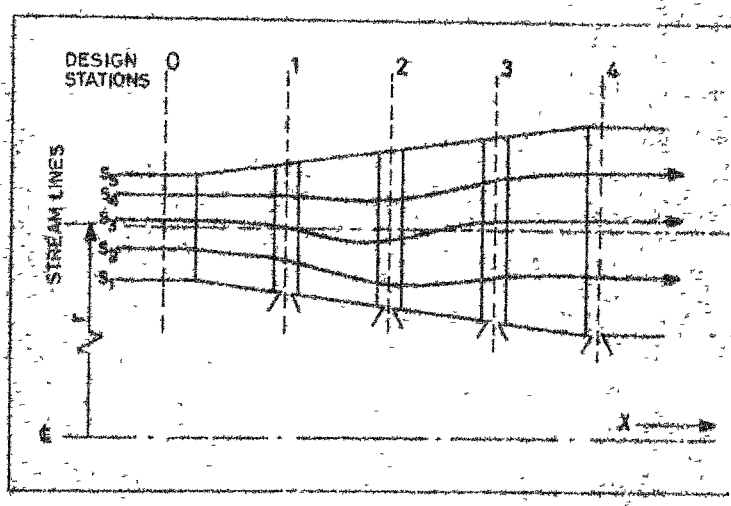

Fig 1a Meridional section of a turbine

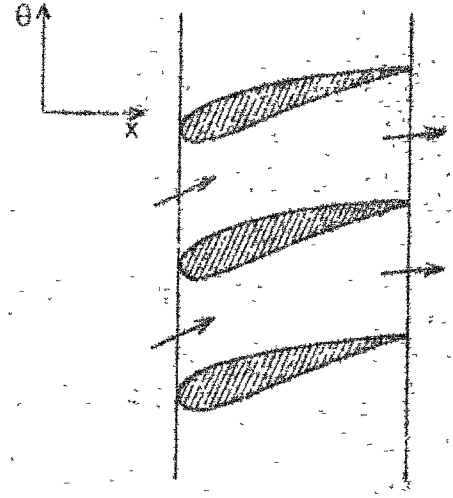

Fig. 1 b Blade to blade section of a turbine

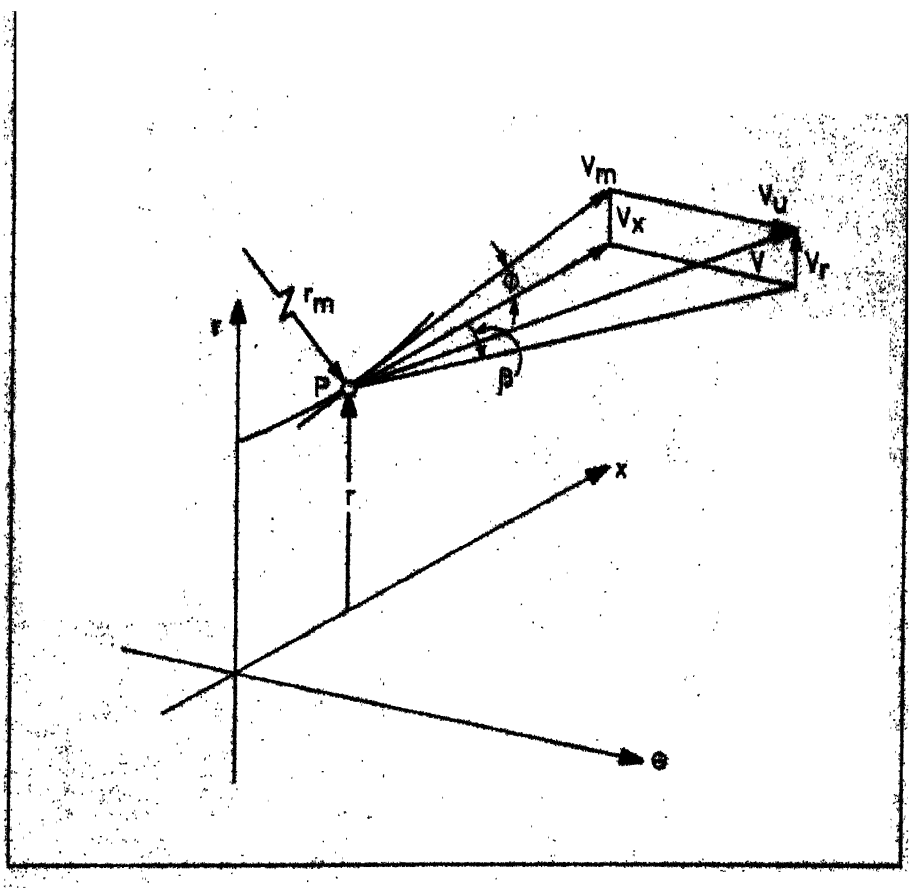

Fig. 2 Nomenclature for the flow

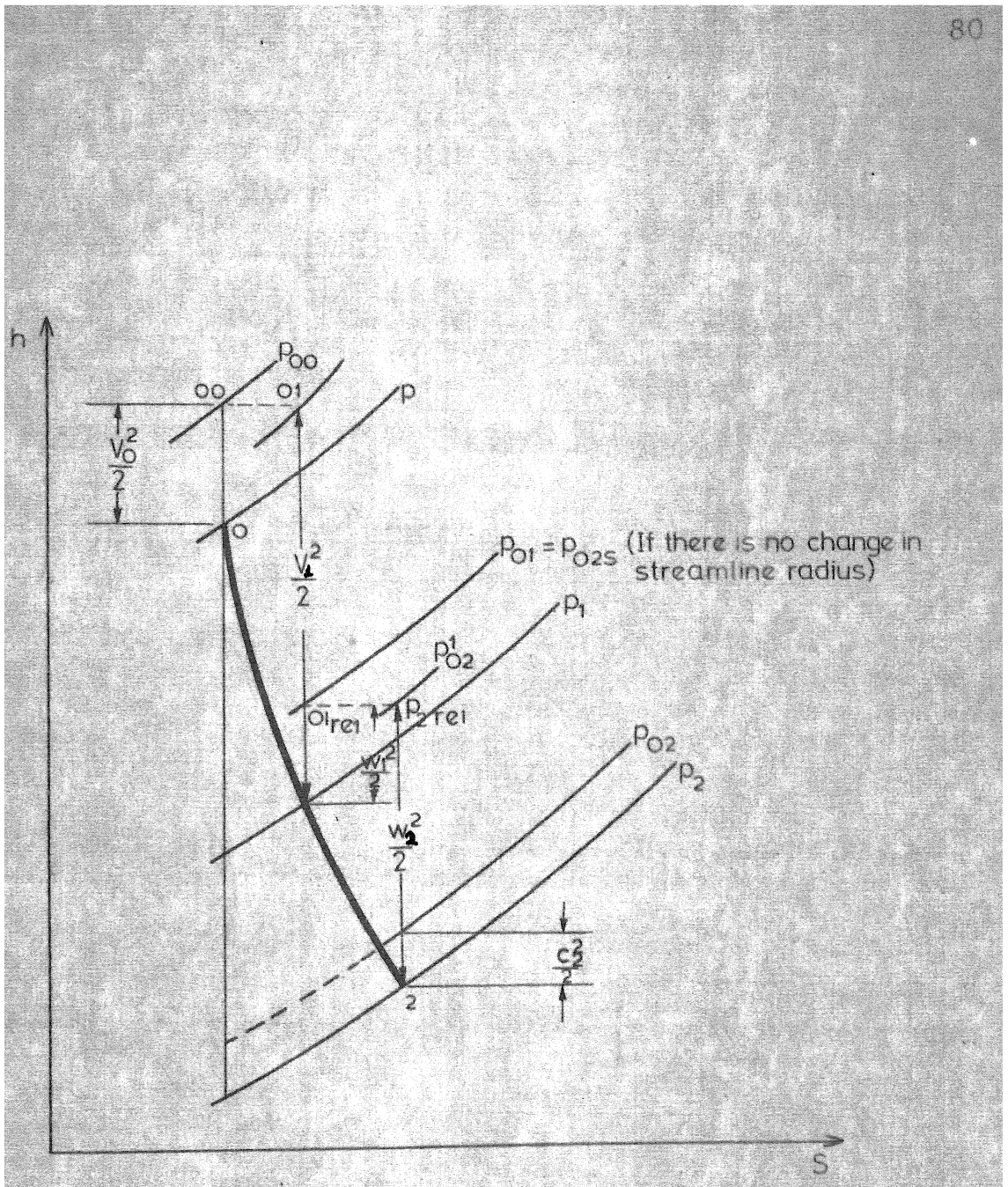

Fig. 3 Enthalpy-entropy diagram for a stage

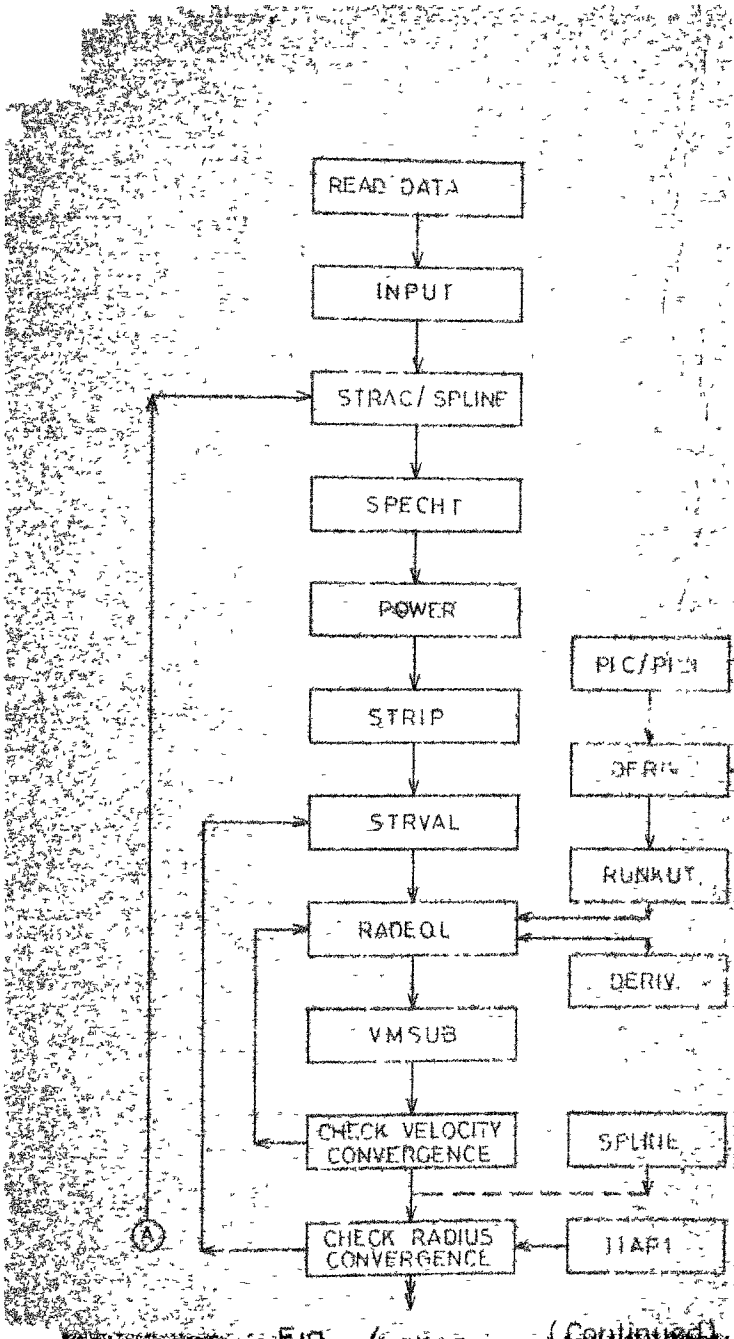

Fig. 4 (Continued)

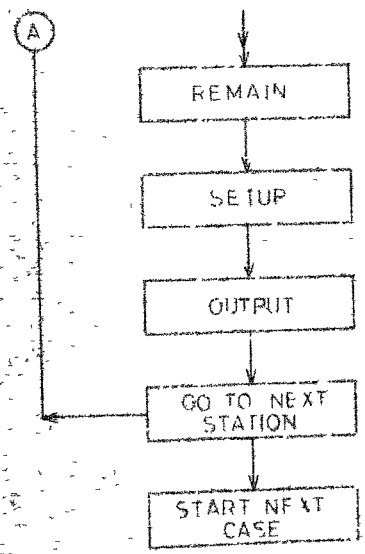

Fig. 4 Flow chart of subroutine callin sequence

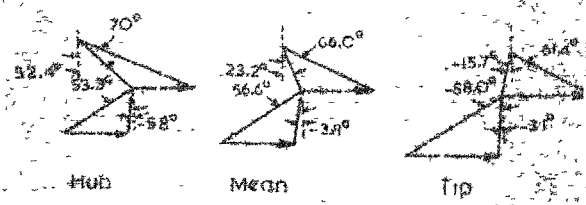

DESIGN VELOCITY DIAGRAMS

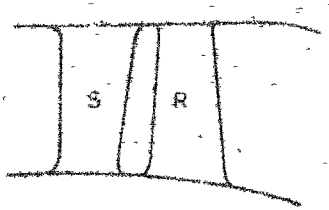

TURBINE FLOWPATH

Fig. 5 (Test case 1)

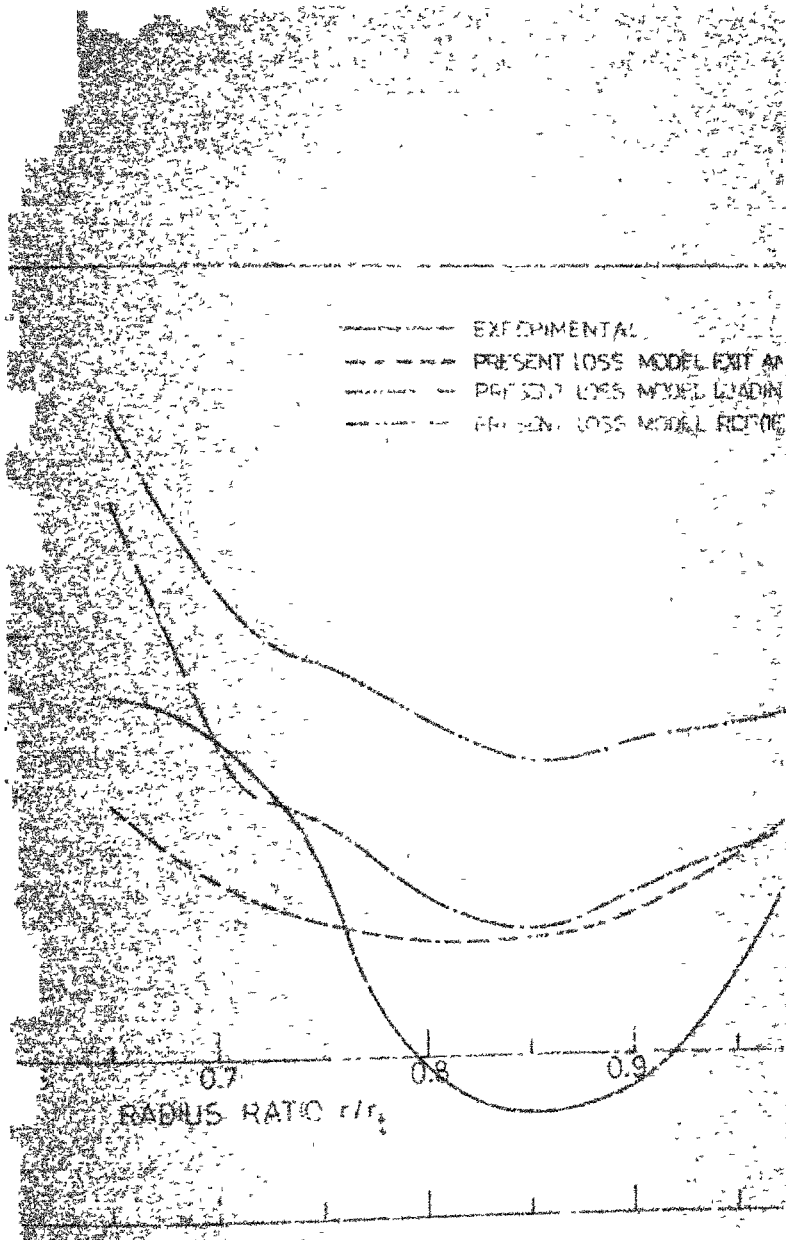

Fig. 6 Outlet flow angle distribution at turbine exit
test case 1.

Stage exit total pressure distribution for

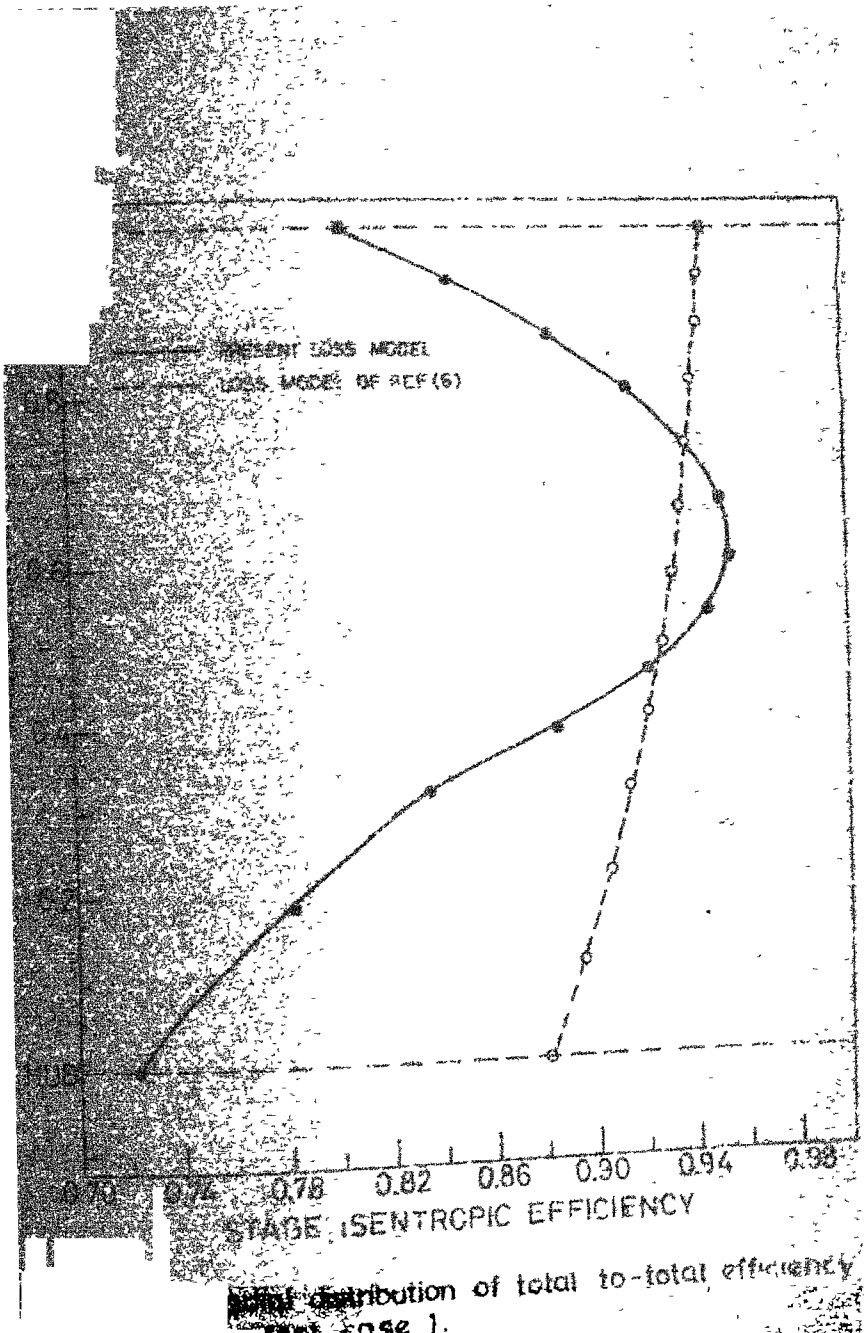

distribution of total to-total efficiency
test case 1.

Fig. 9 Design velocity diagrams (

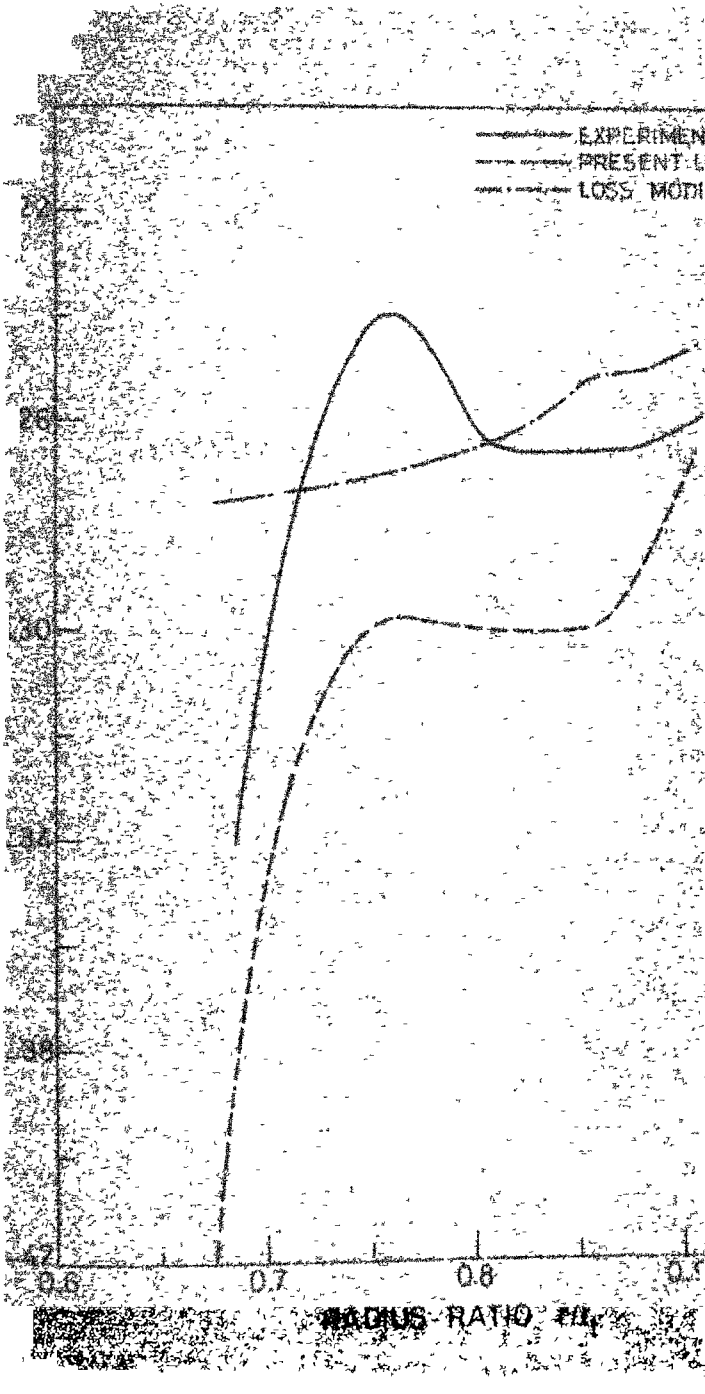
EXPERIMEN
PRESENT
LOSS MODI
0.8
0.7
0.8

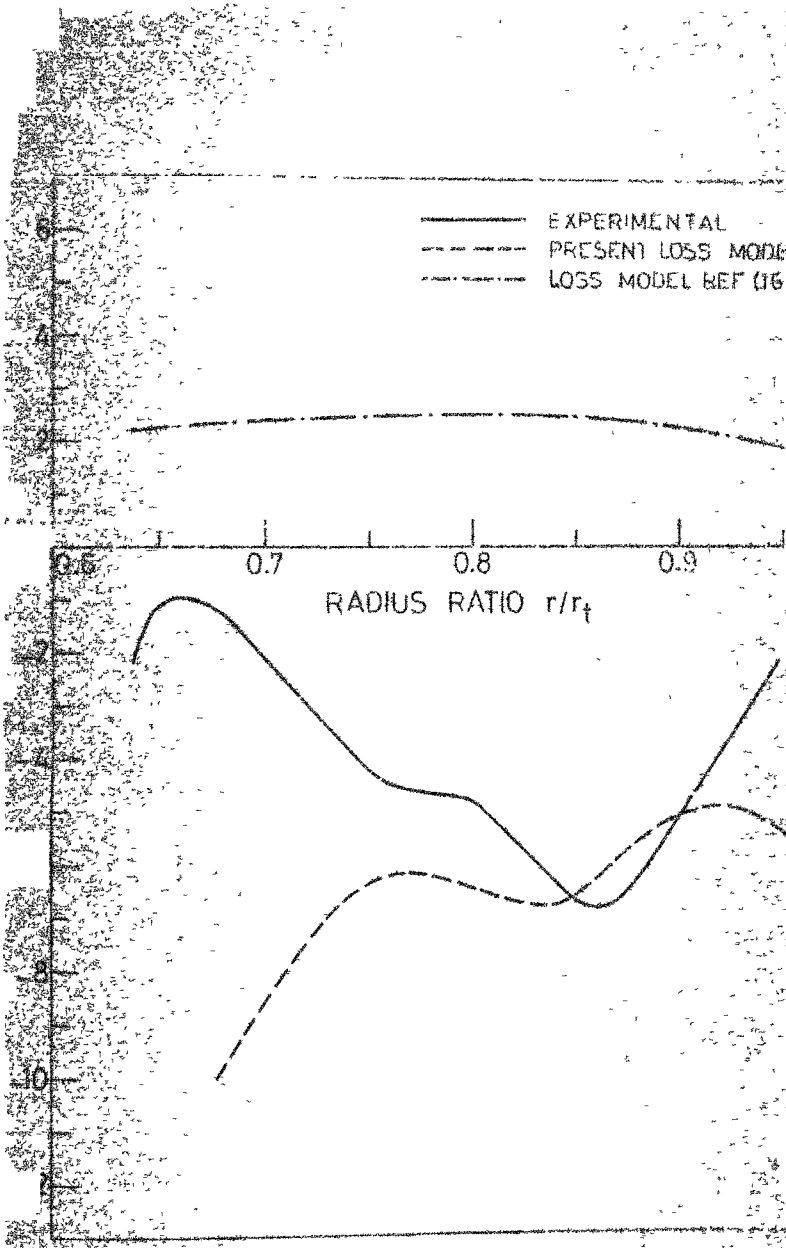

Outlet flow angle distribution at turbine
test case 2.

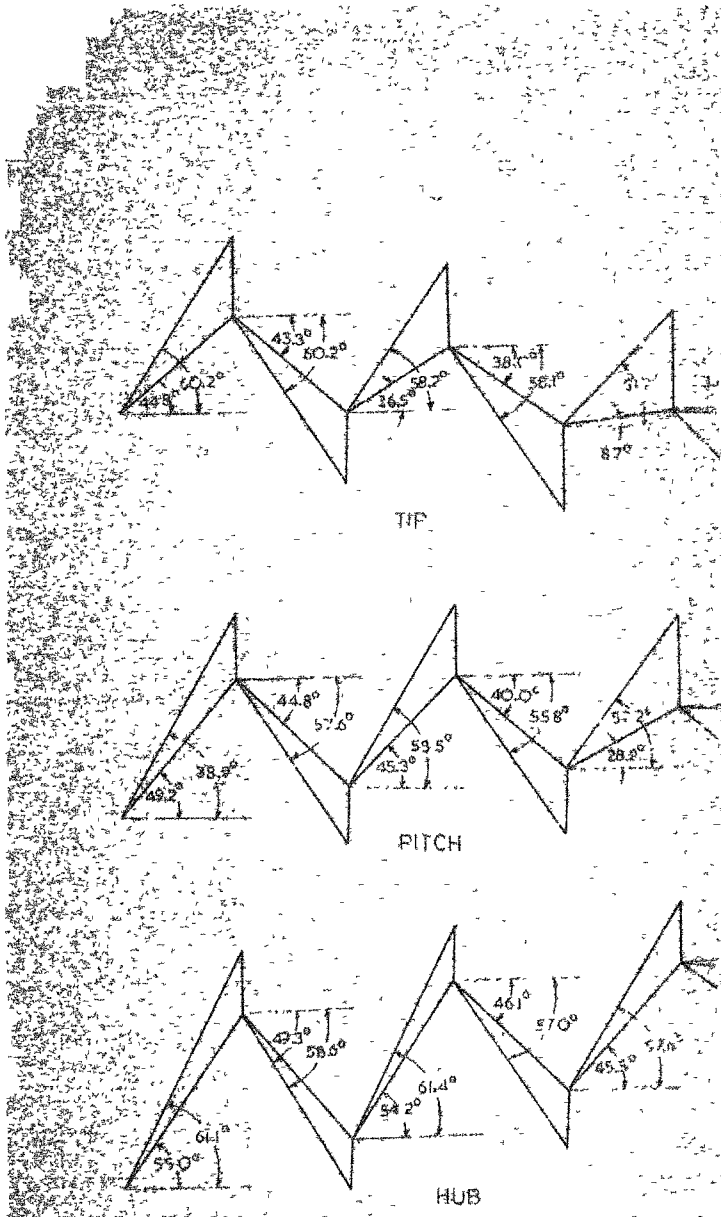

Fig. 7.2 Turbine design velocity diagr

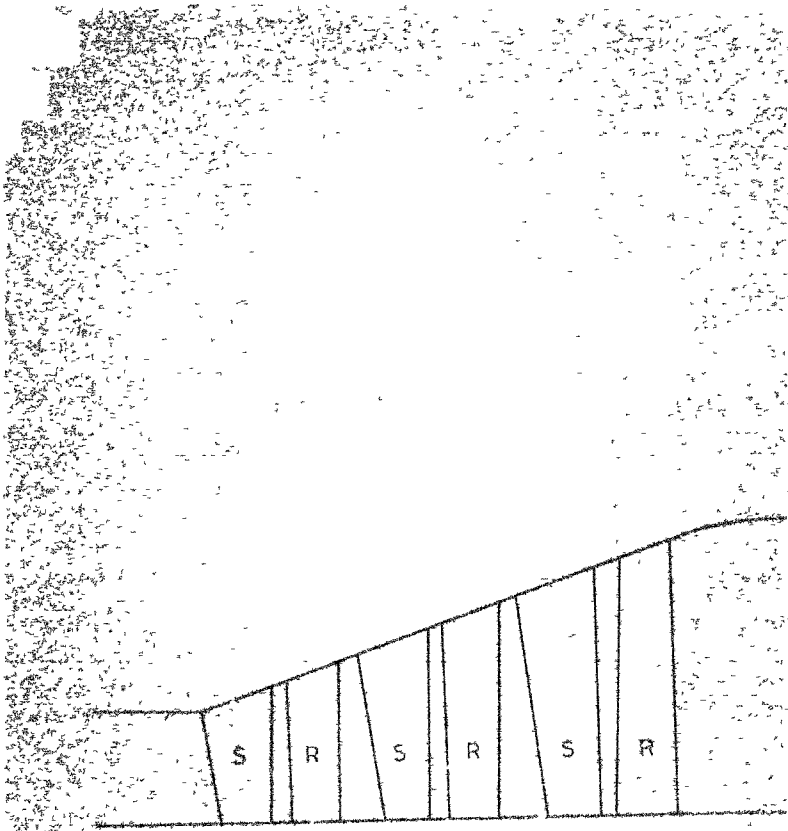

Fig. 12b Turbine flowpath (Test case 3)

PRESENT LOSS MODEL
EXPERIMENTAL
PERCENTAGE BLADE HEIGHT
100
80
60
40
20
0

PERCENTAGE BLADE HEIGHT
100
80
60
40
20
0
0.76
0.80
0.84
0.88
0.92
0.96
TOTAL-TO-TOTAL EFFICIENCY

PRESENT LOSS MODEL
EXPERIMENTAL
PERCENTAGE BLADE HEIGHT
100
80
60
40
20
0

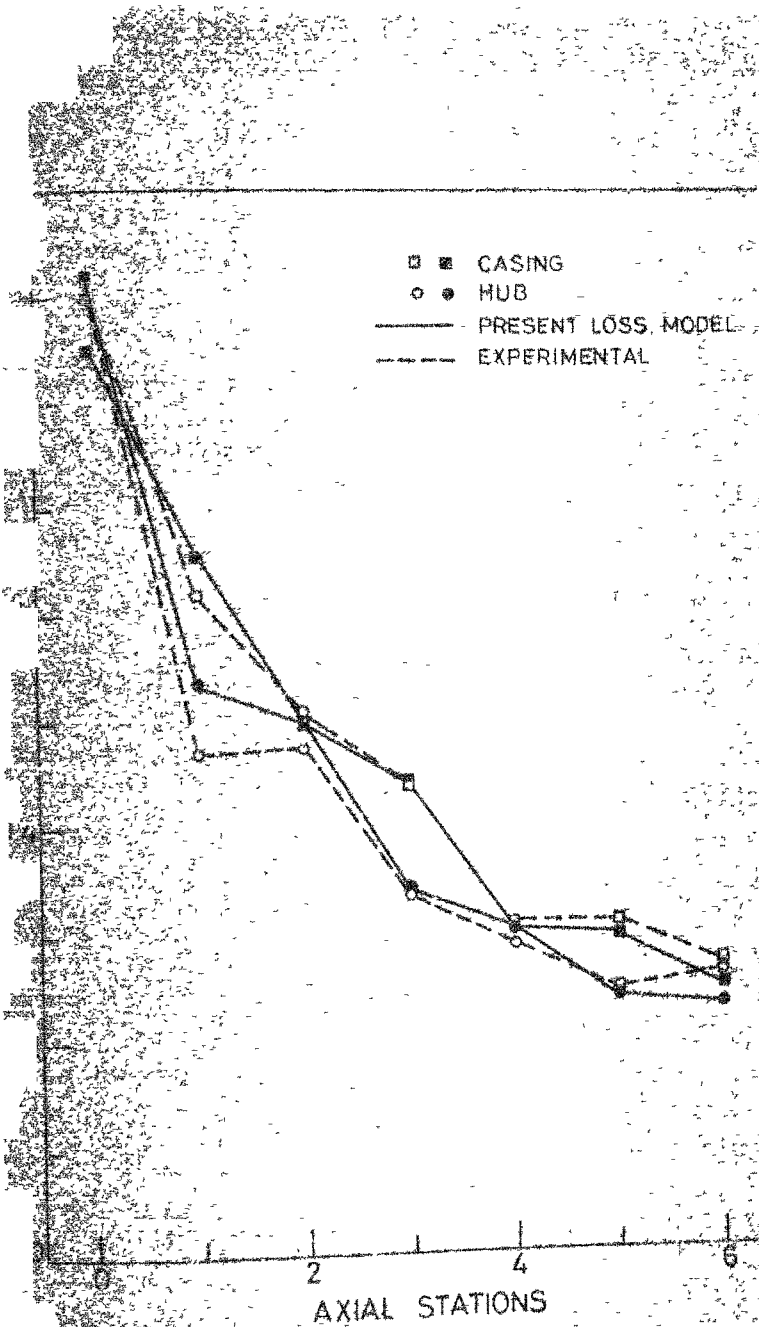

Fig. 11 Wall static pressure distribution for the

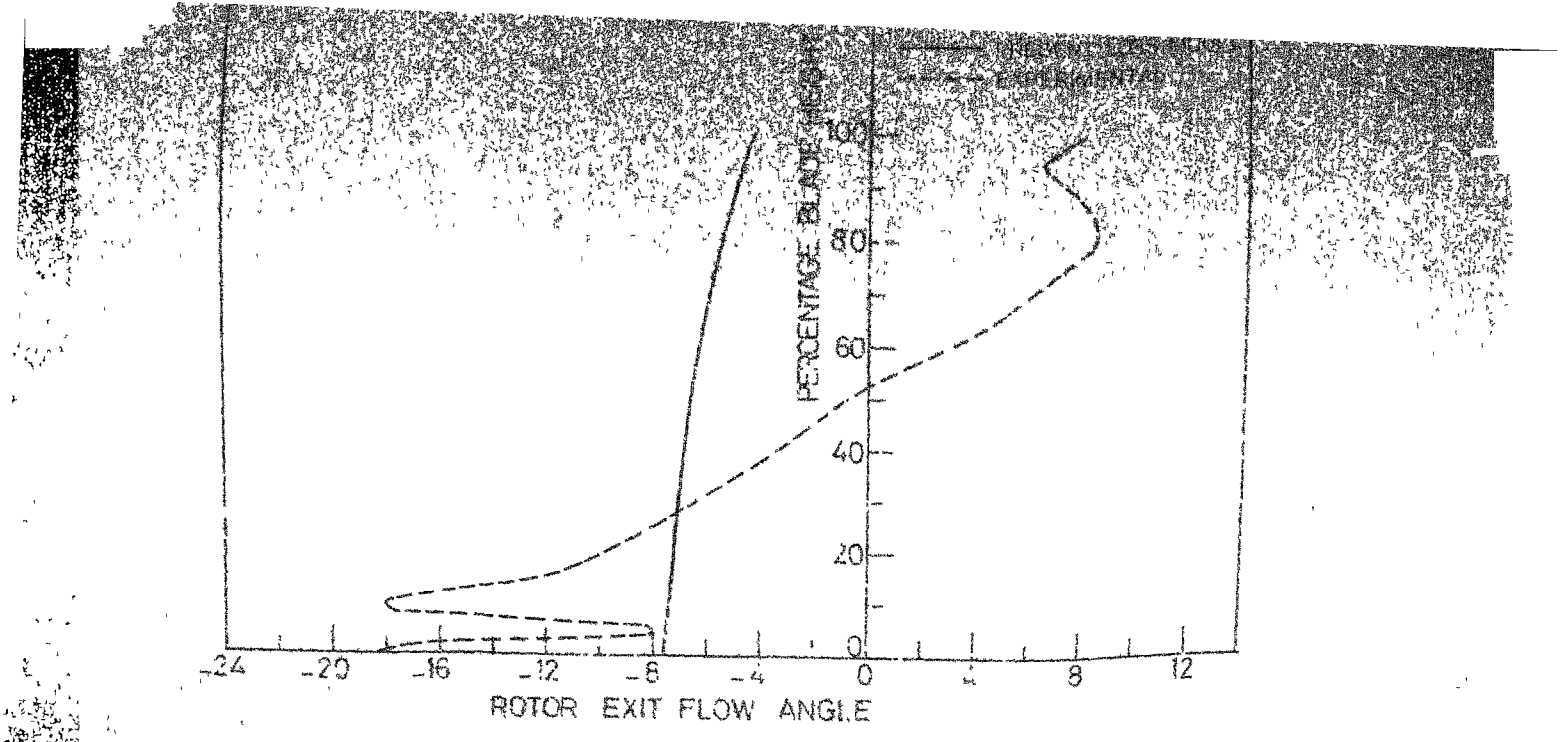

Exit flow angle distribution at turbine exit for test case 3.

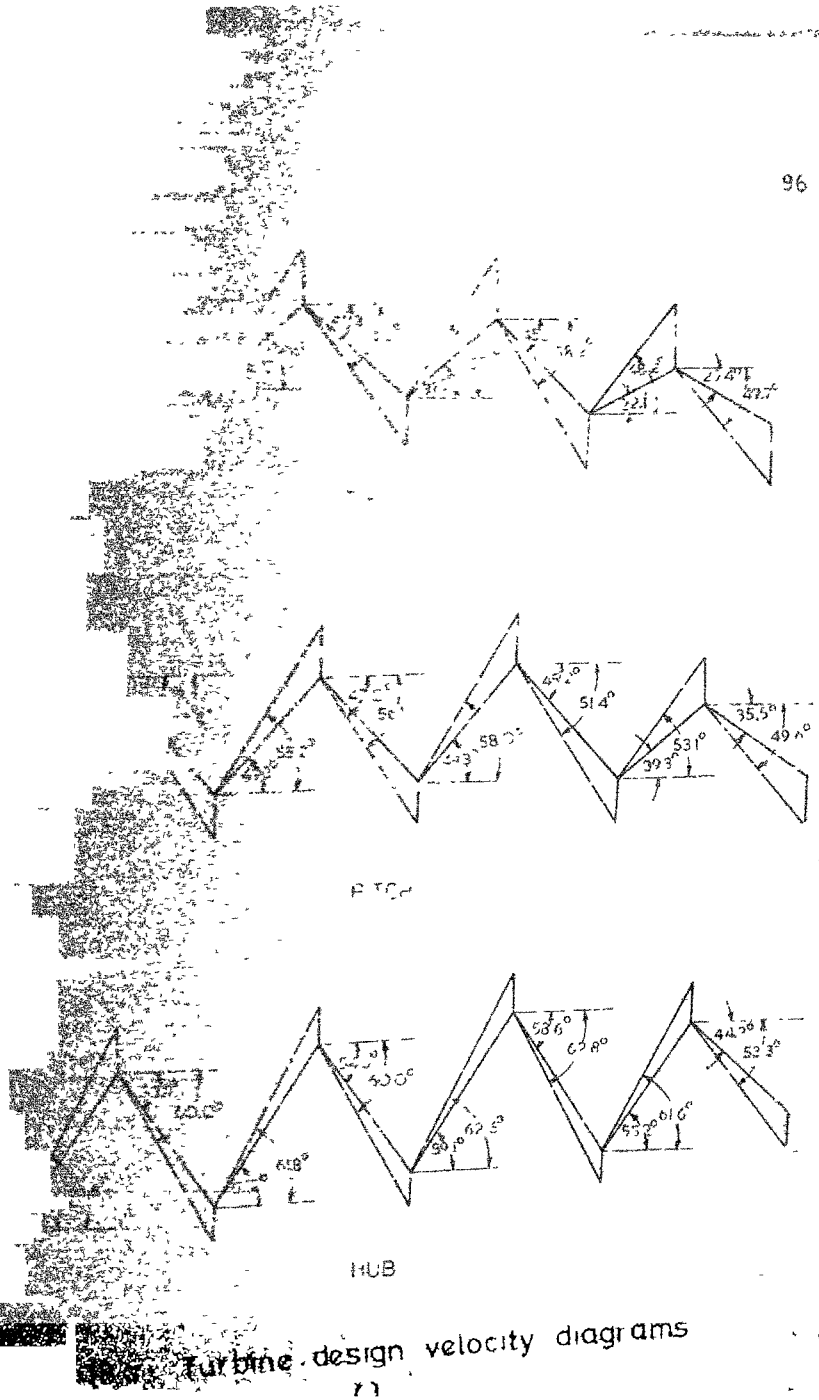

Turbine design velocity diagrams

Fig. 18b Turbine flowpath (Test

PERCENTAGE BLADE HEIGHT
100
80
60
40
20
0
EXPERIMENTAL
PRESENT QUASI 3D MODEL

PERCENTAGE BLADE HEIGHT
100
80
60
40
20
PRESENT LOSS MODEL
EXPERIMENTAL

Fig 23 Outlet total pressure

Fig. 24 Wall static pressure distribution for

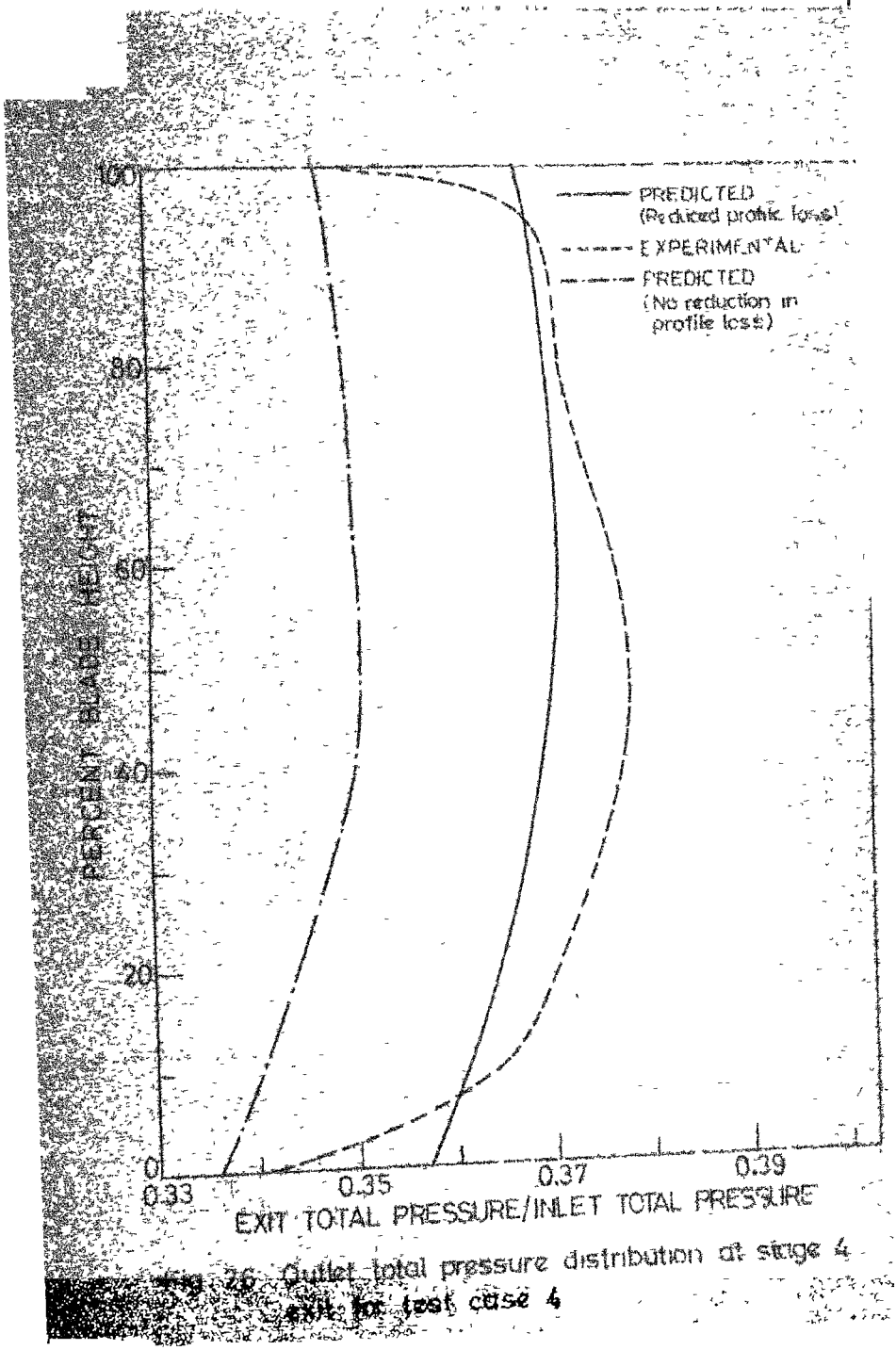

Fig 26 Outlet total pressure distribution at stage 4 exit for test case 4

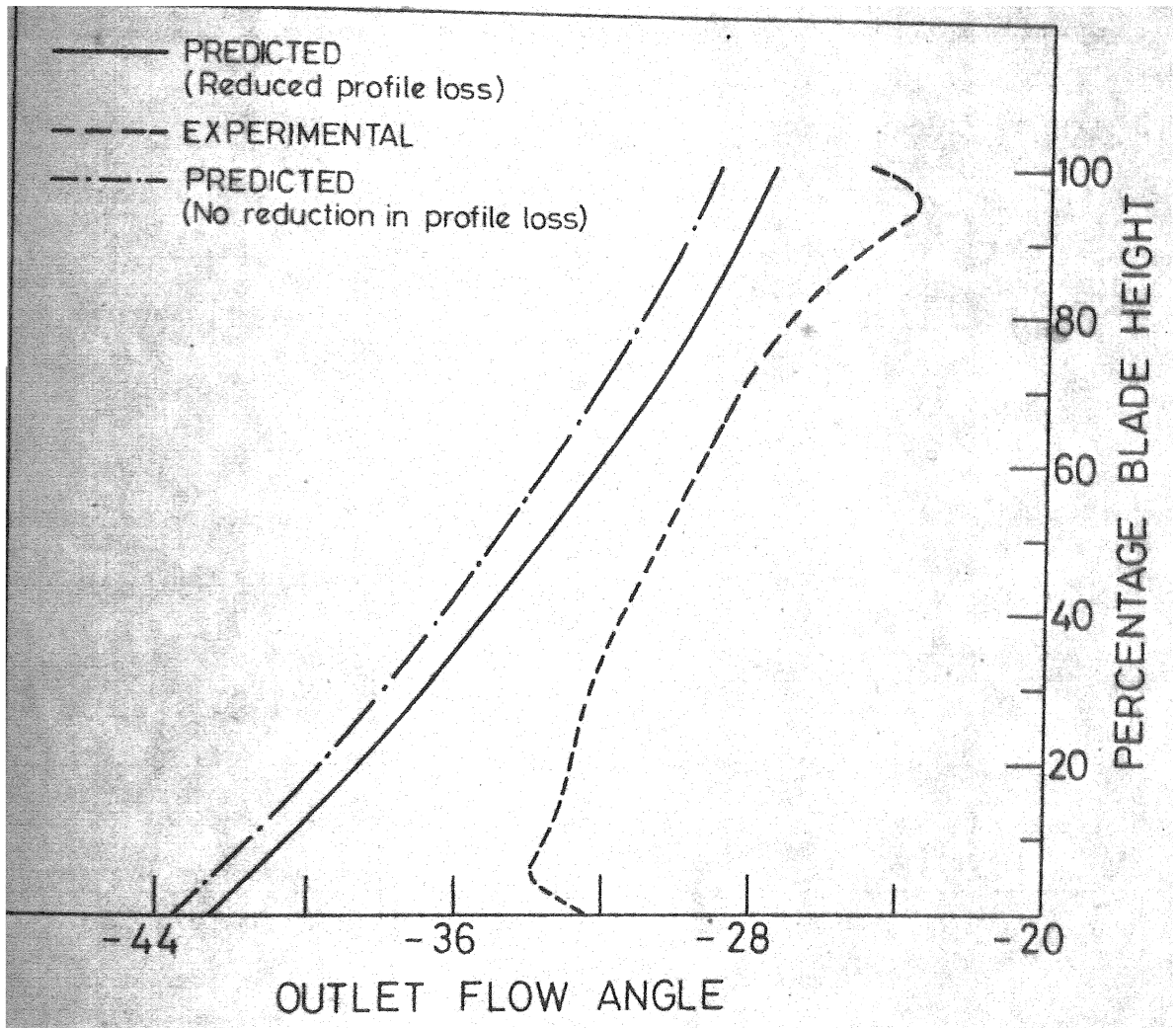

Fig. 27 Outlet flow angle distribution at stage 4 exit for test case 4